

## RESEARCH ARTICLE

# The small GTPase KIRho5 responds to oxidative stress and affects cytokinesis

Marius Musielak<sup>1,\*</sup>, Carolin C. Sterk<sup>1,\*</sup>, Felix Schubert<sup>1</sup>, Christian Meyer<sup>2</sup>, Achim Paululat<sup>2</sup> and Jürgen J. Heinisch<sup>1,‡</sup>

## ABSTRACT

Rho5 is the yeast homolog of the human small GTPase Rac1. We characterized the genes encoding Rho5 and the subunits of its dimeric activating guanine-nucleotide-exchange factor (GEF), Dck1 and Lmo1, in the yeast *Kluyveromyces lactis*. Rapid translocation of the three GFP-tagged components to mitochondria upon oxidative stress and carbon starvation indicate a similar function of KIRho5 in energy metabolism and mitochondrial dynamics as described for its *Saccharomyces cerevisiae* homolog. Accordingly, *Klrho5* deletion mutants are hyper-resistant towards hydrogen peroxide. Moreover, synthetic lethality of *rho5* deletions with key components in nutrient sensing, such as *sch9* and *gpr1*, are not conserved in *K. lactis*. Instead, *Klrho5* deletion mutants display morphological defects with strengthened lateral cell walls and protruding bud scars. The latter result from aberrant cytokinesis, as observed by following the budding process *in vivo* and by transmission electron microscopy of the bud neck region. This phenotype can be suppressed by *KICDC42<sup>G12V</sup>*, which encodes a hyper-active variant. Data from live-cell fluorescence microscopy support the notion that KIRho5 interferes with the actin moiety of the contractile actomyosin ring, with consequences different from those previously reported for mutants lacking myosin.

**KEY WORDS:** Rho-type GTPase, Mitochondrion, Cell wall, Nutrient stress, Yeast

## INTRODUCTION

Small GTPases comprise a huge family of molecular switches, which cycle between a GDP-bound inactive and a GTP-bound active state and thereby regulate essential biological processes from signaling cascades and intracellular protein trafficking to cell motility (reviewed in Takai et al., 2001). Among them, the subfamily of Ras-homologous (Rho) GTPases is widespread within eukaryotes, with the model yeast *Saccharomyces cerevisiae* carrying six members, Rho1 to Rho5 and Cdc42 (Park and Bi, 2007). Rho5 was the last to be identified, then as a negative regulator of cell wall integrity (CWI) signaling (Schmitz et al., 2002a). It is now considered a homolog of human Rac1, which controls actin cytoskeleton dynamics and also affects energy metabolism in mammalian cells,

with its malfunction associated with diverse diseases, including cancer development and neurodegenerative disorders (Eliáš and Klimeš, 2012; Marei and Malliri, 2017). Supporting its homologous function, we found that activation of Rho5 in *S. cerevisiae* depends on a dimeric guanine-nucleotide-exchange-factor (GEF), consisting of Dck1 and Lmo1, the yeast homologs of mammalian DOCK and ELMO proteins (Schmitz et al., 2015).

Further investigations in *S. cerevisiae* underlined the importance of Rho5 as a putative hub for various signal transduction processes (reviewed in Hühn et al., 2019). Thus, besides regulating the CWI pathway, it participates in the regulation of the high-osmolarity glycerol (HOG) pathway (Annan et al., 2008). Rho5 also reacts to glucose starvation by translocating rapidly from the plasma membrane to mitochondria (Schmitz et al., 2018, 2015). An implication in nutrient sensing was also deduced from the synthetic phenotypes of a *rho5* deletion with mutants defective in nutrient signaling components, such as *sch9* and *gpr1* (Schmitz et al., 2018). Large-scale screens further supported such an association, as Rho5 was found to interact with a large number of glycolytic enzymes as well as with Ras1 (Singh et al., 2019a). Rho5 also translocates rapidly to the mitochondria under oxidative stress, depending on its interaction with and activation by both GEF subunits (Sterk et al., 2019). Recent studies further confirmed the involvement of Rho5 in mitochondrial dynamics, as they revealed interactions with Atg21, a central component of autophagy, and Msp1, an outer mitochondrial membrane protein (Singh et al., 2019a). This was in line with previous suggestions of a role for Rho5 in the regulation of yeast mitophagy and apoptosis (Schmitz et al., 2015; Singh et al., 2008). Finally, interactions with major eisosome components such as Pil1 and Sur7 provided additional evidence for its relation to cell surface and cell wall organization, as indicated by the initial genetic studies (Schmitz et al., 2002b; Singh et al., 2019a).

With regard to its domain structure, Rho5 in *S. cerevisiae* shares many features with other eukaryotic GTPases. Thus, it carries the two switch regions required for nucleotide binding and activation, as well as a C-terminal CAAX box as a target for lipid modification and association with the plasma membrane (Sterk et al., 2019). The latter also relies on a conserved polybasic region (PBR), which precedes the CAAX motif. A specific feature of Rho5 in *S. cerevisiae*, as opposed to its human Rac1 homolog, is an extension of 98 amino acid residues upstream of the PBR, which participates in its proper intracellular distribution.

The yeast *Kluyveromyces lactis* is amenable to both classical and molecular genetic techniques developed for *S. cerevisiae*, but relies on a predominantly respiratory rather than a fermentative metabolism (Rodicio and Heinisch, 2013). In broad terms, the physiology of *K. lactis* cells thus mimics that of healthy mammalian cells, whilst the fermentative *S. cerevisiae* would be more similar to cancer cells (Andrejc et al., 2017). The respiratory orientation of *K. lactis* is also reflected in the fact that in cells grown in glucose

<sup>1</sup>Universität Osnabrück, Fachbereich Biologie/Chemie, AG Genetik, Barbarastr. 11, D-49076 Osnabrück, Germany. <sup>2</sup>Universität Osnabrück, Fachbereich Biologie/Chemie, AG Zoologie, Barbarastr. 11, D-49076 Osnabrück, Germany.

\*These authors contributed equally to this work

‡Author for correspondence (jheinisc@uni-osnabrueck.de)

© F.S., 0000-0002-4225-7598; A.P., 0000-0002-8845-6859; J.J.H., 0000-0003-4197-4285

Handling Editor: David Glover

Received 14 December 2020; Accepted 19 August 2021

media, mitochondria are more abundant in images from transmission electron microscopy (TEM) than in *S. cerevisiae*, whilst other features such as the cell wall are alike in the two yeasts (Backhaus et al., 2010). In line with these observations, the p53-dependent generation of reactive oxygen species (ROS) and related apoptotic processes were shown to be independent of the carbon source in *K. lactis*, but only occurred under non-fermentative conditions in *S. cerevisiae* (Kumar et al., 2017).

Despite the similarities in molecular investigations to *S. cerevisiae*, very little information is available on GTPases in *K. lactis*. In fact, as far as Rho-type GTPases are concerned, only KIRho1 has been studied in some detail. It is an essential protein that interacts with protein kinase C (KIPkc1), and is activated by the GEF KIRom2, suggesting that it serves a similar function in CWI signaling as its homolog in *S. cerevisiae* (Lorberg et al., 2003; Rodicio et al., 2006). Non-Rho-type GTPases studied so far in *K. lactis* include Gpa1, the alpha-subunit of the trimeric complex in the mating pheromone pathway (reviewed in Coria et al., 2006), KIRas2, whose role so far has only been studied in relation to mating and mating-type switching (Barsoum et al., 2011), and the eukaryotic initiation factor eIF2 for its function in translation (Llacer et al., 2018). Additional GTPases in *K. lactis* have been described with five septins, which control cytokinesis and are functionally conserved to their counterparts in *S. cerevisiae* (Rippert and Heinisch, 2016). On the other hand, KIMyo1, a component of the constrictive actomyosin ring (AMR), seems to be less important for *K. lactis* than its homolog in *S. cerevisiae*, as *Klmyo1* deletions are perfectly viable, although they are temperature sensitive and display morphological defects at 37°C (Rippert et al., 2014). Nevertheless, in wild-type *K. lactis* cells the dynamics of AMR constriction and the formation of primary and secondary septa follow those known for *S. cerevisiae*, and budding leaves relatively flat scars on the mother cells (Rippert et al., 2014).

Given the medical importance of Rac1 in humans, and the association of Rho5 with oxidative stress response and apoptosis in *S. cerevisiae*, in the present study we decided to study the role of Rho5, and that of its dimeric GEF, in the respiratory yeast *K. lactis*. We showed that, similarly to its homolog in *S. cerevisiae*, KIRho5 responds to both oxidative stress and nutrient limitation by translocating together with its GEF to mitochondria. Yet, genetic interactions with two key components of nutrient sensing, Sch9 and Gpr1, are not conserved in *K. lactis*, probably because of its predominantly respiratory metabolism. Importantly, a lack of KIRho5 activity results in significantly thicker cell walls and in distinct morphological defects caused by an aberrant budding process, which is different from *S. cerevisiae* and reminiscent of Rac1 functions in the organization of the mammalian cytoskeleton.

## RESULTS

### KIRho5 mediates oxidative stress response

Rho5 together with its dimeric GEF, henceforth referred to as the DLR complex, mediates the response to oxidative stress and glucose starvation in the fermentative yeast *S. cerevisiae* (Schmitz et al., 2018, 2015). We wondered whether (1) this complex exists in the more respiratory-oriented yeast *K. lactis* and (2) if its intracellular distribution and physiological function is affected in a similar way under stress. To address the first question, a search for homologous genes with synteny in the yeast gene order browser (<http://ygob.ucd.ie/>), complemented by sequence alignments of the deduced proteins, revealed the presence of homologs of *ScRHO5*, *ScDCK1* and *ScLMO1* in the *K. lactis* genome, with overall amino acid

identities of 47%, 38% and 27%, respectively (see Fig. S1 for alignments). As expected, regions covering putative functional domains of the two GEF subunits, such as the SH3 domain near the N-terminus of KIDck1 and putative sites of interactions, show higher degrees of conservation. The GTPase KIRho5 was also aligned with its human homolog HsRac1, showing 43% amino acid identity, which is significantly higher compared to only 32% between ScRho5 and HsRac1 (Fig. S1). The lower identities with ScRho5 can be attributed to its extension by 98 amino acids, which precedes the C-terminus and serves important functions in the *S. cerevisiae* GTPase (Sterk et al., 2019). This extension is much shorter or completely absent in KIRho5 and HsRac1, respectively (Fig. S1).

Next, the three identified genes were cloned with their flanking regions by PCR from the genome of a *K. lactis* wild-type strain to facilitate their molecular analysis, as outlined in the Materials and Methods section. To confirm that the Rho5 proteins of *K. lactis* and *S. cerevisiae* were functionally equivalent, we employed two independent tests for heterologous complementation. First, either the wild-type *KIRHO5* gene or its activated mutant allele *KIRHO5*<sup>Q69H</sup> was introduced into a recipient strain carrying an *Scrho5* deletion, which confers hyper-resistance towards hydrogen peroxide (Schmitz et al., 2015). As shown in Fig. S2A, the *KIRHO5* alleles both restored the growth sensitivity under oxidative stress in drop dilution assays, in contrast to the empty control vector. In fact, expression of the activated allele provoked a hyper-sensitivity, similar to published data on its *S. cerevisiae* homolog (Sterk et al., 2019). Complementation capacity was also validated for the synthetic lethality of *rho5* null mutants with a *sch9* deletion in *S. cerevisiae* (Schmitz et al., 2018). Introduction of the wild-type *KIRHO5* gene or its activated mutant allele *KIRHO5*<sup>Q69H</sup> into a heterozygous diploid strain (*rho5/RHO5 sch9/SCH9*), followed by sporulation and tetrad analysis, yielded only viable segregants with the double deletion (*rho5 sch9*) if they also carried a plasmid encoding a functional KIRho5 (Fig. S2B).

To assess the physiological role of the putative DLR complex in *K. lactis* (KIDLR), the three genes were individually deleted (Fig. 1A). All three deletions (*Klrho5*, *Kldck1* and *Kllmo1*) produced viable segregants in tetrad analyses, with colony sizes similar to the wild-type segregants on YEPD plates, indicating that KIRho5 activity is not essential (Fig. 1B). Segregants from such analyses were selected for growth assays on rich medium containing hydrogen peroxide, since *Scrho5* deletions are known to be hyper-resistant to this stressor. As evident from Fig. 1C, cells lacking any of the three KIDLR components indeed displayed an increased resistance towards oxidative stress as compared to the wild type.

### *Klrho5* lacks the genetic interactions described for its *S. cerevisiae* homolog and does not affect chronological life span

Since the hyper-resistance of *Klrho5* deletions towards hydrogen peroxide appears to be too moderate to serve as a suitable phenotype for genetic screens, we looked for stronger criteria to perform complementation studies. As stated above, *Scrho5* deletions are synthetically lethal with an *Scsch9* deletion and synthetically sick with *Scgpr1* deletions, attributed to a connection to nutrient sensing (Schmitz et al., 2018). Therefore, we identified the homologs *KISCH9* and *KIGPR1* by synteny analyses and cloned and deleted the respective genes from the *K. lactis* genome (Fig. 2A,B). Segregants carrying a *Klsch9* deletion obtained from a heterozygous diploid strain produced drastically smaller colonies than those of the

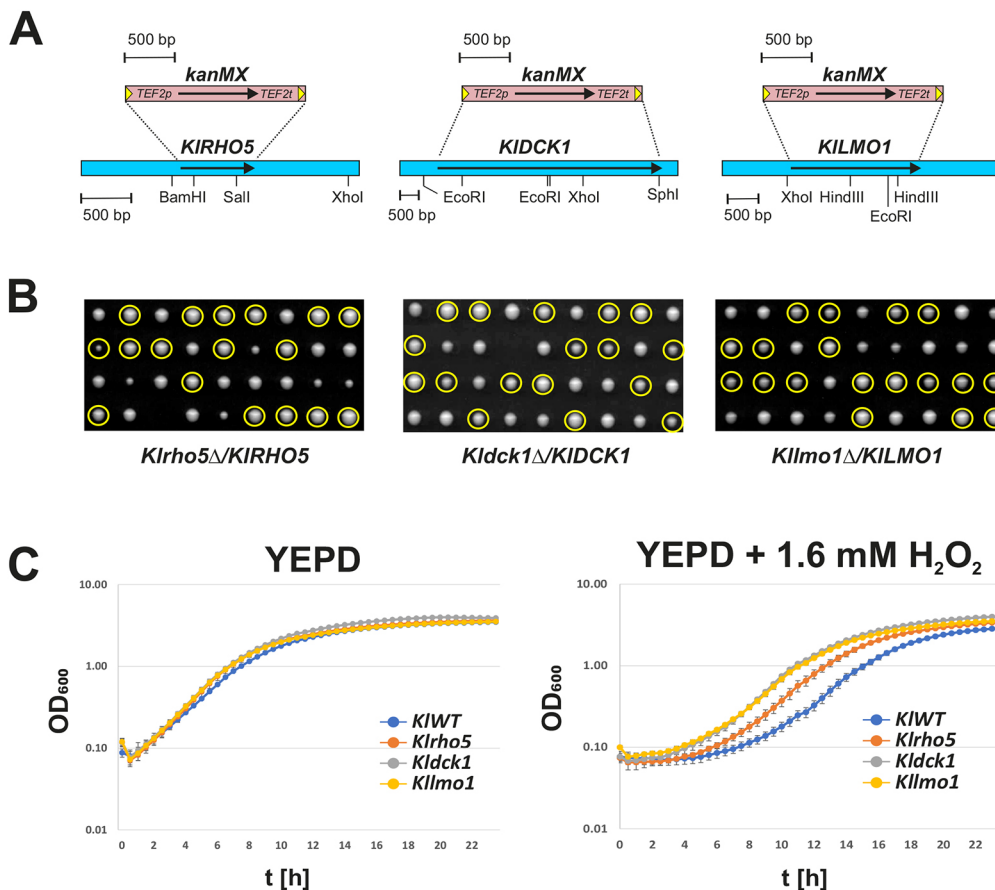


**Fig. 1. Deletions in genes encoding the *K. lactis* DLR complex do not affect growth under standard conditions, but are hyper-resistant towards hydrogen peroxide.**

(A) Schematic representation of the deletion constructs for *KIRHO5*, *KIDCK1*, and *KILMO1*. The *kanMX* cassette was amplified from pUG6 (Geldener et al., 1996) by PCR with appropriate oligonucleotides and used to substitute the respective open reading frames (arrows) by homologous recombination. Some restriction sites in the target sequences are given for orientation. Correct substitution of the open reading frames was verified by PCR with flanking oligonucleotides. (B) The heterozygous diploid strains KHO364, KHO371, and KHO362 were sporulated, subjected to tetrad analyses and allowed to grow for 3 days at 30°C on YEPD plates. Replica plating was used to verify the correct segregation of all genetic markers, with G418 resistance indicating the respective deletions (yellow circles). (C) Strains KHO208-8A (wild type, KIWT), KHO208-8B (*Klrho5*), KHO218-9A (*Kldck1*), and KHO255-3A (*Kllmo1*) were pre-grown in YEPD, adjusted to  $OD_{600}=0.1$  and growth was followed in YEPD without and with 1.6 mM hydrogen peroxide. Three independent biological replicates were measured for each strain and error bars show the s.d. at each time point.

wild type upon germination on YEPD plates (Fig. 2C), whereas strains carrying the *Klpr1* deletion were not affected (Fig. 2D), both reminiscent of the respective deletion strains in *S. cerevisiae* (Schmitz et al., 2018). However, in contrast to *S. cerevisiae*, both the *Klrho5 Klsc9* and the *Klrho5 Klpr1* double deletions were viable, and neither showed an additive phenotype as compared to the segregants with the single deletions (Fig. 2E and F, respectively).

A total of fifteen other gene deletions were tested in attempts to find a synthetic lethality with the *Klrho5* deletion, either in analogy to reported genetic interactions in *S. cerevisiae* or because they seemed plausible in the light of the phenotypes observed herein. These included crosses with strains defective in carbohydrate signaling, the pentose phosphate pathway, oxidative stress response, cell wall synthesis, cytokinesis or DNA repair. As listed in Table S3, haploid segregants carrying the double deletions in combination with *Klrho5* were obtained from tetrad analyses in all cases, with no obvious additive growth phenotypes, i.e. they were neither synthetically lethal nor obviously synthetically sick.

An interesting phenotype reported for an *Scrho5* deletion was a reduced chronological life span in the genetic background of the BY-strain series in baker's yeast (Cao et al., 2016). We therefore assessed the loss of cell viability in stationary phase cells kept in synthetic minimal medium for three different haploid strains, each, carrying either a *Klrho5* deletion or a wild-type *KIRHO5* allele. All strains showed a similar loss of viability over a period of 3 weeks, with no significant differences between wild type and the deletions (Fig. S3), indicating that KIRho5 is not involved in the regulation of chronological life span in *K. lactis*.

### Stress induces the rapid translocation of the KIDLRL complex to mitochondria

Given the differences in primary structures of the three KIDLRL proteins to their homologs in *S. cerevisiae*, and the lack of analogous synthetic interactions, we next addressed the distribution of the trimeric complex in *K. lactis* under different growth conditions to shed some light on their cellular functions. To this end, GFP fusions were constructed for each of the three genes at their original chromosomal loci, expressed from their native promoters. KIDck1-GFP and KILmo1-GFP were obtained as C-terminal fusions, in analogy to their functional *S. cerevisiae* homologs. GFP-KIRho5 was tested as an N-terminal fusion, to prevent interference with the C-terminally located CAAX-box, which is required for proper localization (Fig. S1; Sterk et al., 2019). We noted that the genomic *GFP-KIRHO5* fusion encoded a GTPase that was not fully functional, as judged by the increased appearance of morphologically aberrant cells (see next section). In order to avoid this phenotype, *GFP-KIRHO5* was cloned into a non-replicating vector and integrated at the *K. lactis leu2* locus, leaving the wild-type *KIRHO5* allele at its native chromosomal position intact.

While the GFP-tagged variants of KIDck1 and KILmo1 showed a diffused cytosolic distribution in cells grown under standard conditions, GFP-KIRho5 localized at the plasma membrane, as expected (Fig. 3A; note that KIDck1-GFP and KILmo1-GFP occasionally seem to form patches at internal structures. Closer inspection showed that these signals neither colocalize with a nuclear marker nor with stained vacuoles, as shown in Fig. S4). However, upon addition of hydrogen peroxide, all three signals

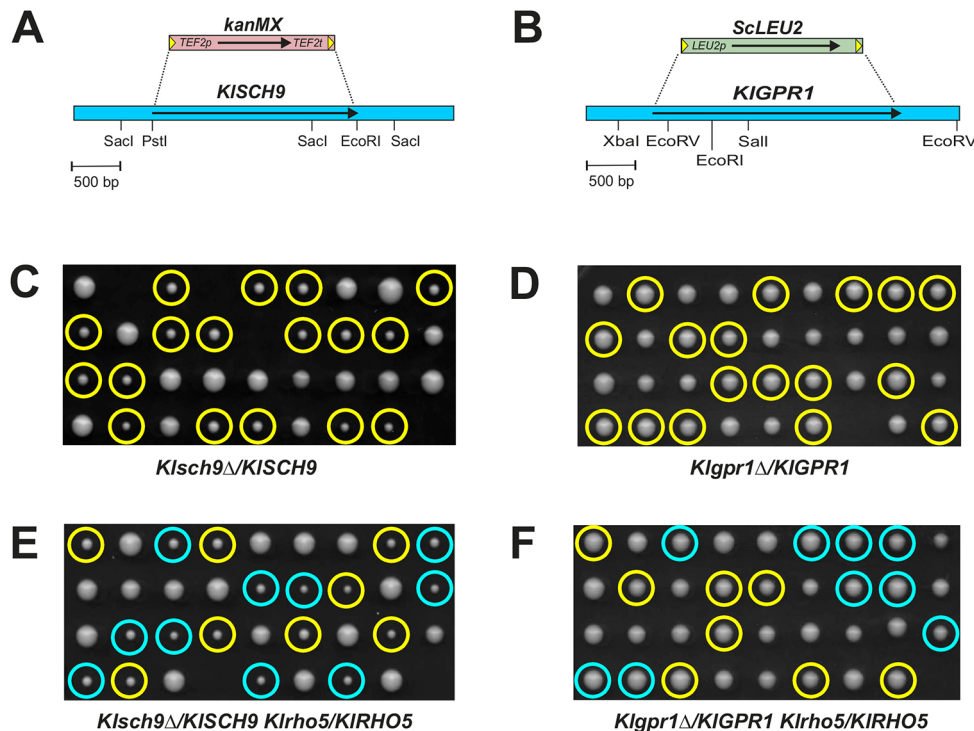


**Fig. 2. Deletions of *KIRHO5* do not genetically interact with those of *KISCH9* and *KIGPR1*.** (A,B) Schematic representation of the deletion constructs for *KISCH9* (A) and *KIGPR1* (B), with some restriction sites in the target sequences given for orientation. The *kanMX* cassette was amplified from pUG6 (Guedener et al., 1996); for the *ScLEU2* cassette, pJH955L (Heinisch et al., 2010) was used as template. Primer pairs carried >40 nucleotides of homology to the flanking regions of the target genes and 20 nucleotides homologous to the respective template plasmid. Transformants were selected either on plates with rich medium containing 100 mg/l G418 for the *Klsch9* deletion, or on synthetic medium lacking leucine for the *Klgpr1* deletion. Correct substitution of the open reading frames was verified by PCR with flanking oligonucleotides. (C,D) The diploid strains KHO393 and KHO402 heterozygous for the deletions indicated were sporulated and subjected to tetrad analyses on YEPD plates. Segregants were allowed to grow for 3 days at 30°C. Note that *Klsch9* deletions (yellow circles in C) show a distinct growth retardation, as do their counterparts in *S. cerevisiae* (compare Fig. S2 and Schmitz et al., 2018). No correlation to colony size was observed for *Klgpr1* deletions (yellow circles in D). (E,F) To test for synthetic interactions, strains carrying a *Klsch9* (E) or a *Klgpr1* (F) deletion were crossed to a *Klrho5* deletion to obtain the heterozygous diploid strains KHO401 and KHO384, respectively. They were sporulated and subjected to tetrad analyses on YEPD plates. Segregants were allowed to grow for 3 days at 30°C. Note that the *Klrho5* deletion allele of one parental strain for KHO401 carried a *Klrho5::SpHIS5* allele instead of the *kanMX* marker depicted in Fig. 1A, in order to facilitate the identification of both gene deletions in segregants by replica plating. Yellow circles indicate segregants carrying the single deletions of *Klsch9* and *Klgpr1*, respectively. Blue circles indicate segregants with an additional *Klrho5* deletion.

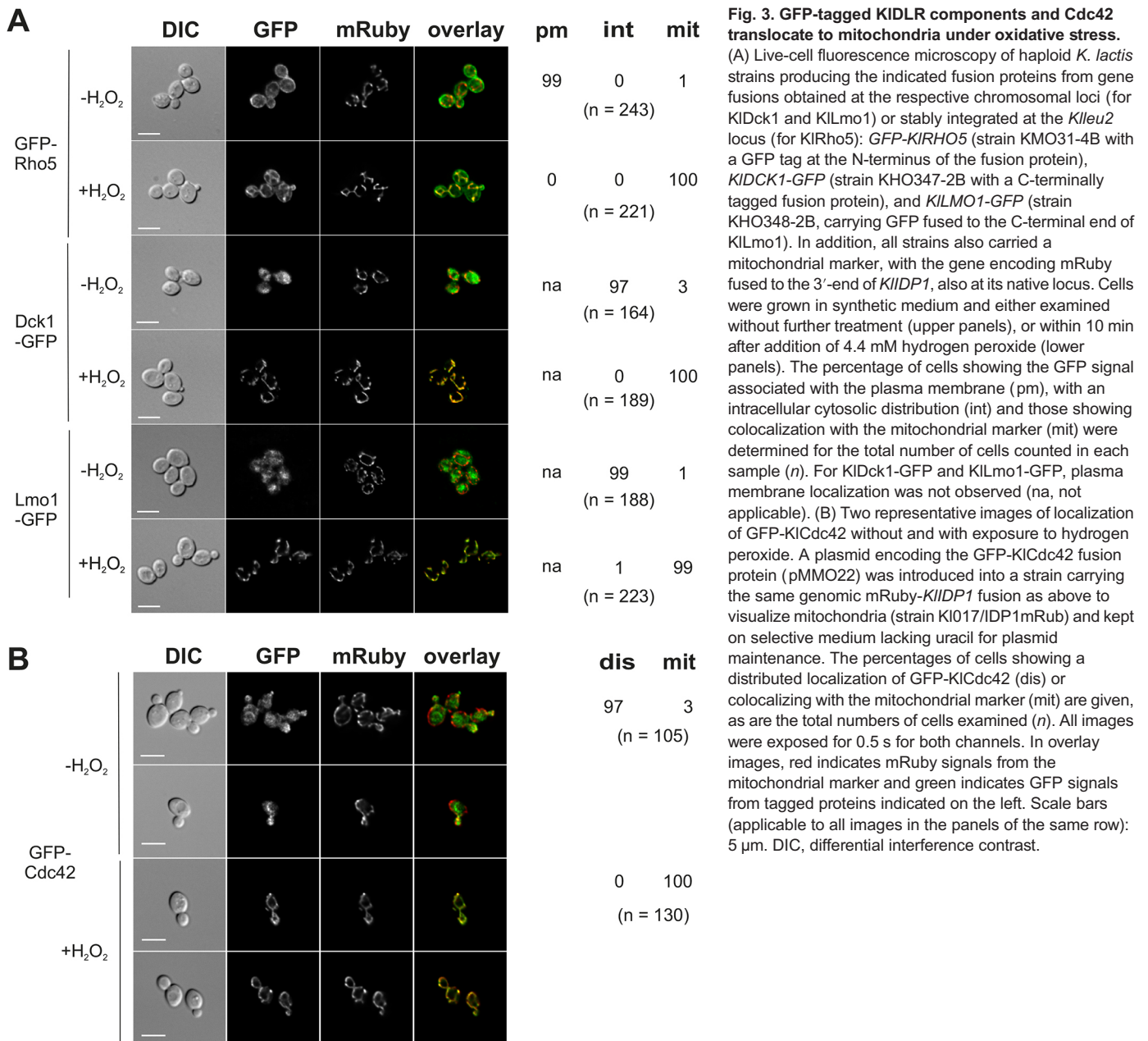
appeared at the mitochondria within the 2–3 min needed to prepare the samples for microscopy. Thus, all three *K. lactis* DLR components translocated like their *S. cerevisiae* homologs, indicating a conserved function in oxidative stress response (Schmitz et al., 2015).

Cdc42, another member of the Rho-GTPase family, which is involved in polarity establishment and morphogenesis in *S. cerevisiae* (Woods and Lew, 2019), has been shown to serve overlapping functions with Rho5 homologs in different filamentous fungi (reviewed in Hühn et al., 2019). Therefore, we assessed the intracellular localization of a GFP-KICdc42 fusion. Under standard growth conditions in *S. cerevisiae*, this GTPase accumulates at the growing bud tip and is associated with the surface of vacuoles and other intracellular membranes (Woods and Lew, 2019). As shown in Fig. 3B, GFP-KICdc42 also translocated efficiently to mitochondria when cells were exposed to hydrogen peroxide, indicating that it indeed could serve a complementary function to KIRho5. This notion was further supported by the suppression analyses of the morphological defects in a *Klrho5* deletion as discussed in the next section. As a note of caution, it should be mentioned that the GFP-KICdc42 fusion construct was not functional, since it did not rescue the lethality of a *Klcdc42* deletion as deduced from tetrad analysis of a suitable heterozygous diploid strain (*Klcdc42::kanMX/KICDC42 GFP-KICDC42::KILEU2/Klleu2*; data not shown).

In accordance with the observations in *S. cerevisiae*, the tagged DLR components of *K. lactis* also quantitatively associated with mitochondria upon glucose starvation (Fig. 4). Thus, despite the metabolic differences between the highly fermentative baker's and the respiratory-driven milk yeast, glucose starvation has a similar effect on the association of Rho5 with mitochondria in both.

### The KIDL complex is required for proper budding

While experimental evidence gathered so far indicates that lack of Rho5 in baker's yeast only moderately affects the number of actin patches per cell (Schmitz et al., 2018), we were intrigued to find a distinct morphological phenotype in cells with a *Klrho5* deletion. As shown in Fig. 5A, most cells carrying the *Klrho5* deletion, but not those of the wild type, had protruded bud scars ('humps') in addition to new middle- to large-sized buds. Similar protrusions were found in strains carrying *Kldck1* and *Kllm1* deletions (Fig. 5A), indicating that lack of KIRho5 activity causes these morphological defects. To confirm that this phenotype was not caused by a second-site mutation in the genetic background of the strains employed, we first introduced the respective wild-type genes on *K. lactis* centromeric vectors. This only led to partial reversion of the phenotype, i.e. a lower percentage of cells with protrusions as compared to the deletion strain carrying an empty vector (data not shown). We assumed that the partial recovery was because of an



insufficient plasmid stability in the respective transformants, previously deduced from the poor transmission of centromeric vectors through meiosis in tetrad analyses in several *K. lactis* strains (Rippert et al., 2014). Therefore, the wild-type *KIRHO5*, *KIDCK1* and *KILMO1* genes were cloned into integrative vectors (pMMO5, pMMO7 and pMMO6, respectively) and inserted by homologous recombination at the *Klleu2* locus into the corresponding deletion strains (KHO277-3D *rho5*; KHO254-1A *dck1*, KHO255-1B *lmo1*). Microscopic inspection revealed that 99% (*n*=209), 98% (*n*=103), and 94% (*n*=118) of the respective cells displayed wild-type morphologies. In contrast, more than 70% of cells from all recipient strains, or those carrying the empty vector integrated at the *Klleu2* locus, had protrusions.

To assess possible overlapping functions with KIRho5 regarding the morphology, we constructed an activated allele of *KICDC42*, encoding a G12V substitution in the GTPase on an integrative vector, and inserted it at the *Klleu2* locus. The resulting strain was

crossed with *Klrho5* deletions and subjected to tetrad analyses. Out of 21 segregants with the double-mutant genotype *Klrho5 KICDC42*<sup>G12V</sup> examined under the microscope, 18 were found to grow like the wild type. This strongly indicated that *KICDC42*<sup>G12V</sup> can suppress the aberrant cell morphology associated with the *Klrho5* deletion.

In an attempt to further substantiate these findings, we also constructed deletions in genes encoding the putative GEF KICdc42 and the scaffold protein KIBem1 in a diploid *K. lactis* strain, since both proteins are related to regulation of morphogenesis mediated by Cdc42 in *S. cerevisiae*. As with the heterozygous *Klcdc42* deletion, segregants from tetrad analyses carrying the respective deletion alleles did not produce colonies, indicating that both genes are essential (Fig. S5A–C). Similar results were also obtained with a heterozygous *Kliqg1* deletion, whose homolog encodes a key regulator of cytokinesis in *S. cerevisiae* (Fig. S5D). Further analyses of gene functions in all these cases were impeded by the fact that we

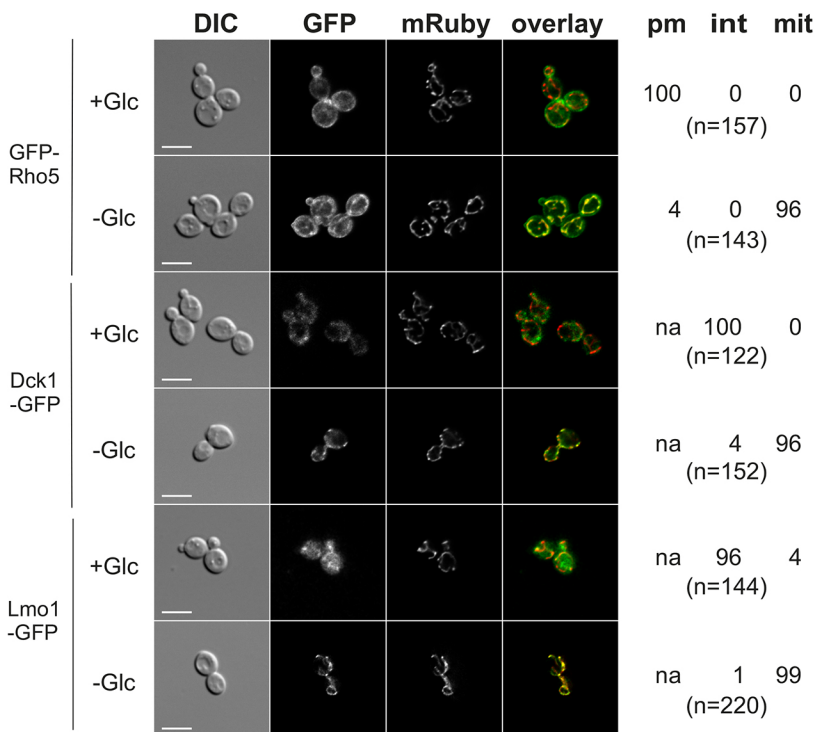


**Fig. 4. GFP-tagged KIDLR components translocate to mitochondria upon glucose starvation.** Localization of GFP-Rho5 (strain KMO31-4B), Dck1-GFP (strain KHO347-2B) and Lmo1-GFP (strain KHO348-2B) relative to the mitochondrial Idp1-mRuby marker under standard growth conditions with 2% glucose (+Glc) and 15 min after transfer to fresh medium lacking glucose (-Glc). Percentages of cells showing localization of the GFP signals at the plasma membrane (pm), in the cytosol (int) or at mitochondria (mit) was quantified as described in the legend of Fig. 3. In the overlay images, red indicates mRuby signals from the mitochondrial marker and green indicates GFP signals from the tagged proteins indicated on the left. Scale bars (valid for all images in the same row): 5  $\mu$ m. DIC, differential interference contrast; na, not applicable.

still lack a tightly regulated promoter for conditional gene expression in *K. lactis* (Rippert et al., 2014).

Two mechanisms may explain the formation of the protrusions in cells lacking active KIRho5: (1) abortive budding, i.e. cells trying to form a bud get stalled and initiate the formation of a new bud at another site, or (2) defective cytokinesis, i.e. the bud neck may be unusually elongated prior to cell separation and thus leave a ‘hump’. In order to distinguish between these possibilities, time-lapse images of growing cells from a *Klrho5* deletion strain were produced and compared to wild-type cells (Fig. 5B; Movies 1 and 2), which showed that indeed the protrusions are remnants of previous budding events, rather than resulting from aborted ones. The same was true for *Kldck1* and *Kllmo1* deletions (Fig. 5B and time-lapse Movies 3 and 4).

To study these structural defects in more detail, we investigated the morphology of the aberrant protrusions by TEM. As summarized in Fig. 5C, *Klrho5*, *Kldck1* and *Kllmo1* deletions frequently produced a distorted primary septum, either bending into the developing bud or not being properly closed, while the wild-type controls displayed regular and fairly straight primary and secondary septa, as described previously (Rippert et al., 2014). In *S. cerevisiae*, secondary septa are deposited from both mother and daughter cells on to the primary septa. Assuming that *K. lactis* follows a similar strategy, a compensatory deposition of excessive glucan may explain the elongation of the bud necks in the mutants, which can ultimately be detected even by light microscopy (Schmidt et al., 2002). Moreover, the strengths of the lateral cell walls were determined from TEM images by measuring lateral cell wall thickness at ten points in each of 14 cells (Fig. 6). While the wild type yielded mean values of  $\sim 85$  nm, all three mutants lacking the KIDLR components increased in thickness to 98 nm, 105 nm and 112 nm for *Kllmo1*, *Kldck1* and *Klrho5* strains, respectively. This indicates that KIRho5 activity is not only required for proper synthesis of the primary septum during cytokinesis, but also participates in the general regulation of cell wall biosynthesis.

The observed protrusions of the bud scars strongly suggested that spatial and/or temporal control of cytokinesis is impaired in mutants in which KIRho5 is either absent or cannot be activated. Given the role of the human Rac1 homolog in the organization of the actin cytoskeleton, we therefore combined strains producing KILifeAct-mRuby and KIMyo1-mCherry fusions, as markers for the contractile AMR, with the GFP-KIRho5 fusion and performed live-cell fluorescence microscopy. KIRho5 accumulated at the bud neck during the late stages of cytokinesis. Thus, an accumulation was observed at the bud neck of cells with large buds, colocalizing with KILifeAct (Fig. 7A). On the other hand, the KIRho5 signal was distributed in patches throughout the plasma membrane of both mother and daughter in cells with small buds, thus colocalizing in this region with KIMyo1 upon its appearance (Fig. 7B; Fig. S6). It should be noted that at the neck of small-budded yeast cells KIRho5 was present, but only accumulated in cells with larger buds, i.e. during later stages of cytokinesis. Pearson coefficients were determined to substantiate these findings (see example images in Fig. 7 and Fig. S6). On average, values of  $0.44 \pm 0.22$  (mean  $\pm$  s.d.) were obtained in a total of 22 images examined for the colocalization of GFP-Rho5 with KIMyo1-mCherry, and  $0.54 \pm 0.10$  ( $n=8$ ) for the colocalization of the GTPase with actin in large-budded cells. In contrast, actin patches in mother and daughter cells did not notably colocalize with GFP-KIRho5. These findings support a role of KIRho5 in the regulation of cytokinesis in *K. lactis*, which probably is exerted after constriction of the AMR. This function is either less pronounced or not shared by its baker's yeast homolog, ScRho5 (Schmitz et al., 2018).

## DISCUSSION

In the present study, we provide evidence that Dck1, Lmo1 and Rho5 can form a functional unit in *K. lactis*, which corresponds to the *S. cerevisiae* DLR complex and to human Rac1 in its association with the dimeric GEF DOCK/ELMO. The identified coding sequences are most probably true homologs of the *S. cerevisiae* genes in *K. lactis*, since they are syntenic in their chromosomal

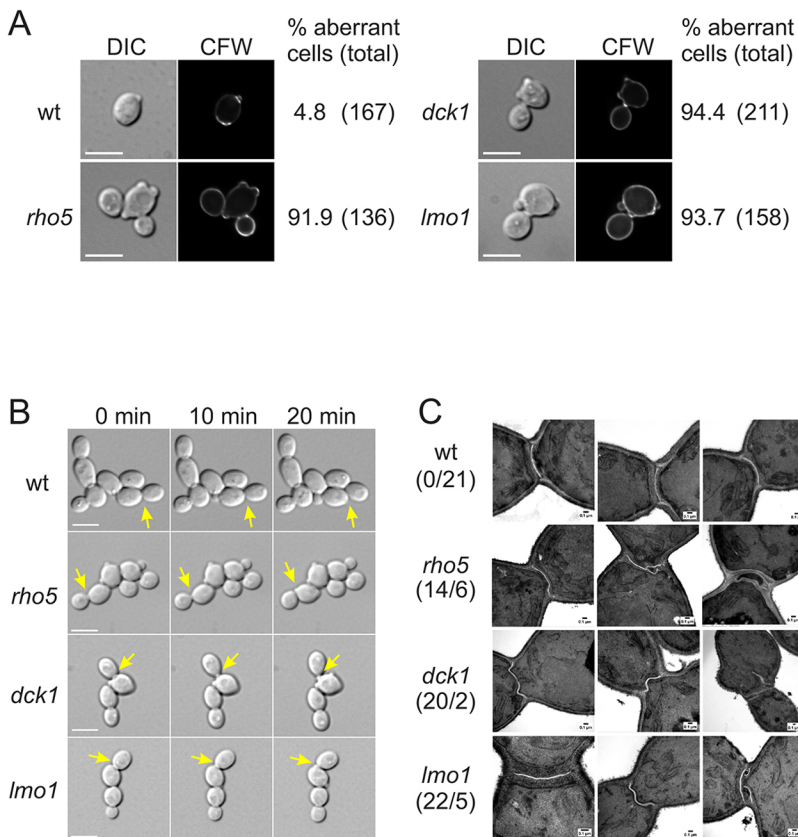


**Fig. 5. Deletion of genes encoding the KIDLR complex causes morphological defects.** (A) Representative images of cells from wild-type (wt, strain KHO208-8A), a *Klrho5* deletion (strain KHO208-8B), a *Kldck1* deletion (strain KHO218-9A) and a *Kllmo1* deletion (strain KHO255-3A) stained with Calcofluor White (CFW) and obtained as differential interference contrast (DIC) bright field images or with fluorescence in the CFW channel with 0.5 s exposures. Numbers to the right give the percentages of cells showing one or more protruding bud scars from total cell counts given in parentheses. Scale bars: 5  $\mu$ m. (B) Selected images from time lapse series obtained from the wild-type strain (wt) and the indicated *K. lactis* deletion mutants. Budding was followed for 20 min each. Yellow arrows indicate sites of budding resulting in protruding bud scars in the mutants. Scale bars: 5  $\mu$ m. (C) Representative images obtained by TEM of budding yeast cells. The numbers in parentheses indicate the ratio of aberrant to normal primary septa in the cells investigated. Strains employed were: CBS2359 (wild type, KIWT), KHO208-8B (*Klrho5*), KHO.01-14C (*Kldck1*) and KHO.03-1D (*Kllmo1*). Scale bars (in the boxes at the lower right corners): 0.1  $\mu$ m.

context and alignments of the deduced amino acid sequences revealed a high conservation, especially when focused on known functional domains. This bioinformatic evidence indicating a functional conservation is strongly supported by our heterologous expression studies, which showed complementation of the *rho5* deletion in *S. cerevisiae* by two variants of *KIRHO5*. With regard to the GTPase, the hypervariable region preceding the C-terminal end is of special interest. For ScRho5, a proper intracellular distribution and an adequate response to oxidative stress depends on the insertion of 98 amino acids, which is not present in the human homolog Rac1, upstream of the C-terminally located PBR sequence, where Rac1 cannot complement the yeast defects (Sterk et al., 2019). In contrast, the functional complementation by KIRho5 in *S. cerevisiae*, whose extension comprises only 44 amino acid residues, indicates that a few conserved residues upstream of the PBR may suffice to render the GTPase active and fully functional in yeasts. We speculate that the extension of the positively charged region retained in the *K. lactis* sequence, especially the KPQKS motif preceding the PBR, may contribute to the interaction with the negatively charged phospholipids and thereby to the membrane association of KIRho5, in analogy to other Ras- and Rho-type GTPases (Fig. S1; Lam and Hordijk, 2013; Williams, 2003). This notion is supported by the fact that human Rac1 can at least partially complement the *Scrho5* deletion, if its C-terminus is replaced by the one of the extended ScRho5 (Sterk et al., 2019).

Another indication of functional conservation of the DLR complex in *K. lactis* is the rapid translocation of all three proteins to mitochondria after exposure to oxidative stress, and their similar physiological response when compared to *S. cerevisiae* (Schmitz et al., 2015). Thus, both *Klrho5* and *Scrho5* deletions, as well as those in the genes for the GEF subunits, provoked a hyper-resistance

towards hydrogen peroxide. In general, *K. lactis* can withstand much higher concentrations of  $H_2O_2$  than *S. cerevisiae*, probably because of its more respiratory lifestyle accompanied by higher production of ROS (Lamas-Maceiras et al., 2015; Santomartino et al., 2019). In *S. cerevisiae*, the increased resistance of mutants lacking DLR complex components was correlated to an impairment of mitophagy and a reduced apoptosis (Schmitz et al., 2015). In this context, it is important that we did not find an effect of a *Klrho5* deletion on the chronological lifespan, in contrast to a report on *Scrho5* (Cao et al., 2016). However, we were not able to reproduce the reduction in CLS for a *Scrho5* deletion in the genetic background of the *S. cerevisiae* strain routinely used in our laboratory (unpublished results), indicating that it may be either strain dependent or very sensitive to minor changes in experimental conditions.

There are also pronounced similarities in the response of Rho5 to glucose starvation in the two yeast species. Thus, the DLR complex quantitatively translocates to mitochondria under such conditions both in *S. cerevisiae* (Schmitz et al., 2018), and in *K. lactis*, as shown herein. However, none of the synthetic phenotypes observed for *Scrho5* in conjunction with deletions in genes involved in nutrient sensing, such as *sch9* or *gpr1*, appears in *K. lactis*. This can be attributed to the fact that *K. lactis* is a Crabtree-negative yeast that does not switch to fermentative metabolism in the presence of high glucose concentrations (reviewed in Rodicio and Heinisch, 2013). Consequently, key regulators of central carbohydrate metabolism, such as the SNF1 complex and its downstream transcription factors KICat8 and KISip4, have been embedded into different regulatory networks as compared to *S. cerevisiae* (Mehlgarten et al., 2015; Mojardin et al., 2018). One of the physiological results of this rewiring is the repression of ethanol utilization by glycerol as a non-fermentable carbon source, which is not observed in *S. cerevisiae*

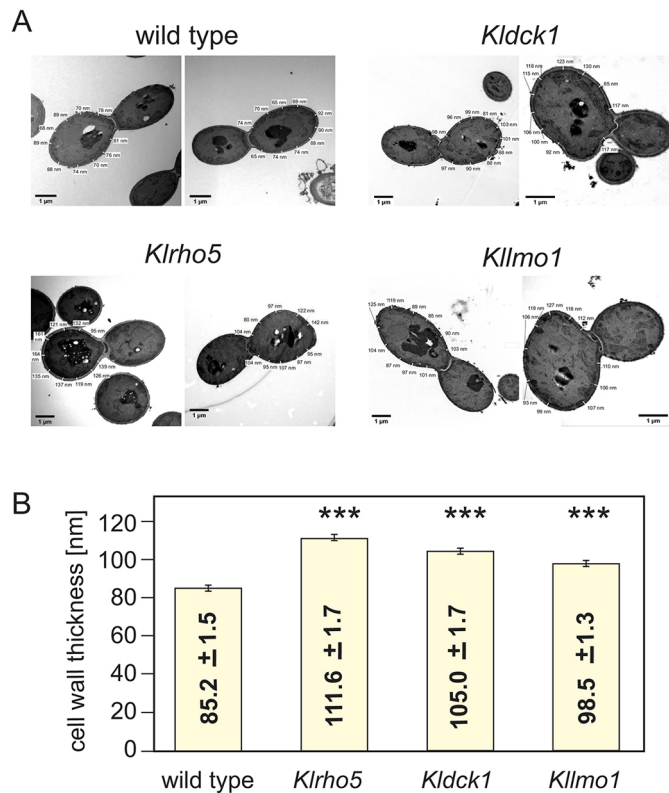


**Fig. 6. Cell wall strength increases in *K. lactis* strains lacking any of the DLR components.** TEM images taken for assessment of the structure of the primary septum were also employed to determine the thickness of the lateral cell wall. (A) For this purpose, thickness was measured in a total of 14 cells for each strain at ten different points, as indicated in the two representative images for each strain. Strains used were: CBS2359 (wild type), KHO208-8B (*Klrho5*), KHO.01-14C (*Kldck1*) and KHO.03-1D (*Kllmo1*). (B) Mean values of cell wall thickness for each strain are given with the respective s.e.m. Differences between the mutants and the wild-type strain are statistically significant, with a *P*-value much smaller than 0.001 (\*\*\*) using the two-sided *t*-test of Microsoft Excel.

(Rodicio et al., 2008). Thus, either KIRho5 is not involved with the regulatory circuits governed by KISch9 and KIGpr1 in contrast to their *S. cerevisiae* counterparts, or, if the genetic interactions are retained, they produce less severe phenotypes not reflected in the growth characteristics tested herein. Addressing these questions would require detailed metabolic studies of the *Klsch9* and *Klgpr1* deletion mutants, which are beyond the scope of this work, but offer interesting perspectives for future investigations.

Most importantly, we found that cells lacking KIRho5 activity display morphological defects not observed in *S. cerevisiae* (Schmitz et al., 2018). The data presented herein indicate that KIRho5 is involved in the regulation of cytokinesis and accumulates at the bud neck after constriction of the AMR. We previously showed that cytokinesis in *K. lactis* basically relies on the same structural and regulatory components as that in *S. cerevisiae*, i.e. a constricting AMR controlled by Hof1 and Cyk3, as well as the septins that form the bud-neck compartment (Rippert and Heinisch, 2016; Rippert et al., 2014). The assembly of septins and AMR constriction are also central events in mammalian cytokinesis and as such essential for human health (Mangione and Gould, 2019). Interestingly, Rac1 in its association with DOCK/ELMO regulates the dynamics of the actin cytoskeleton in mammalian cells (reviewed in Singh et al., 2019b). While this function seems to be poorly conserved in *S. cerevisiae* (Schmitz et al., 2018), our data

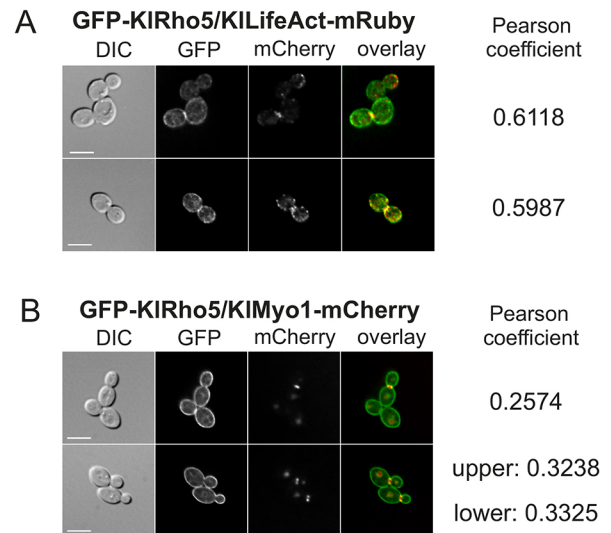


**Fig. 7. GFP-Rho5 accumulates together with the components of the actomyosin ring at the bud neck during cytokinesis.** (A) Representative images of colocalization of GFP-Rho5 with LifeAct-mRuby at budding sites in strain KHO46-6C/2751. (B) Colocalization of GFP-Rho5 with Myo1-mCherry at budding sites in strains KMO30-4A (upper panel) and KMO30-6D (lower panel). See Fig. S6 for more images and colocalization data. Pearson coefficients are given for the cells where both fluorescent markers appear at the bud neck. In the overlay images, red indicates the mRuby (A) and mCherry (B) signals from the tagged proteins indicated above, and green indicates GFP signals from the tagged KIRho5 protein. Images are representative of at least 100 cells inspected in each case. Scale bars (valid for all images in the same row): 5  $\mu$ m. DIC, differential interference contrast.

indicate that KIRho5 may be required for proper cytokinesis in *K. lactis*. As a consequence, closure of the primary septum and deposition of the secondary septa are deregulated in the deletion mutants, and aberrant cytokinesis leads to protruding bud scars retained on the mother cell surface. This is somewhat reminiscent of the filamentous fungus *Eremothecium gossypii* (formerly known as *Ashbya gossypii*), where *rho5* mutants were also shown to produce aberrant septa (Nordmann et al., 2014). It is noteworthy that the protruded bud phenotype observed in the *Klrho5* deletion is different from the multiple buds produced by a *Klmyo1* deletion, which also interferes with proper cytokinesis (Rippert et al., 2014). This indicates that it is the actin moiety of the AMR that is affected by the lack of KIRho5. This view is also substantiated by the observation that accumulation of KIRho5 at the bud neck occurred after AMR constriction, when KIMyo1 was no longer detectable.

In *S. cerevisiae*, the homolog of mammalian IQGAP, Iqg1, is recruited together with actin to the bud neck after deposition of myosin II (Lippincott and Li, 1998). Interestingly, both activated Rac1 and Cdc42 can bind to IQGAPs in mammalian cells (Nouri et al., 2020; Ozdemir et al., 2018). This offers the intriguing possibility that KIRho5 and KICdc42 may control the recruitment of actin to the bud neck in *K. lactis* during cytokinesis by interacting with KILqg1. The GTPases could then be activated to participate in the control of cell wall synthesis, especially the primary septum. It will be interesting to follow up these associations in future research.

Consistent with a conserved role in the negative regulation of cell wall synthesis through CWI signaling (Schmitz et al., 2002a), *Klrho5* deletions also displayed an increased thickness of the lateral cell walls. In conclusion, while the influence of Rho5 on the actin cytoskeleton could have degenerated in the fermentative baker's yeast as compared to Rac1, it seems to be retained from mammalian cells to fungi in general, and especially in the respiratory-oriented



yeast *K. lactis*. This is a further example of why *K. lactis* in many cases may be a better eukaryotic model system than *S. cerevisiae*, as previously proposed for the study of tauopathies related to Alzheimer's disease (Heinisch and Brandt, 2016).

## MATERIALS AND METHODS

### Strains and growth conditions

Yeast strains employed and their genotypes are listed in Table S1. All strains were derived from the congeneric series described previously (Heinisch et al., 2010), which is based on the sequenced *K. lactis* type strain CBS2359. Yeast cell culture and genetic techniques followed standard procedures (Rose et al., 1990). Rich medium (YEPD) contained 1% yeast extract, 2% Bacto Peptone (Difco Laboratories Inc., Detroit, MI, USA) and 2% glucose. Synthetic media were prepared as described in Rose et al. (1990), with the omission of amino acids or bases as required for selection of plasmids or deletion markers and 2% glucose (SCD). For selection of the *kanMX* marker, 100 mg/l of G418 was added to the medium after sterilization.

For serial drop-dilution assays, cells were grown overnight at 30°C in SCD to late logarithmic phase, diluted in fresh medium to an OD<sub>600</sub> of 0.1, grown for another 3 h and subjected to 10-fold serial dilutions. A 3 µl aliquot of each dilution was spotted on to the indicated media and plates were incubated for 3 days at 30°C. Images were scanned and adjusted for brightness and contrast using Corel Photo Paint with the same settings for the entire plate, prior to compilation of lanes into the final figures. Growth curves were obtained in 100 µl cultures in 96-well plates, in YEPD with or without hydrogen peroxide as indicated, and recorded in a Varioskan LUX plate reader (Thermo Scientific, Bremen, Germany) as described previously (Sterk et al., 2019).

*K. lactis* strains were crossed on malt agar plates (5% malt, 3% agar), incubated for 2 days at 30°C and replica plated on to appropriate synthetic media for selection of diploids. For tetrad analyses, diploid strains were grown to late logarithmic phase in liquid YEPD, collected by centrifugation (10,000 g for 1 min at room temperature) and dropped on to 1% potassium acetate plates for sporulation at 30°C. After 1–2 days and microscopic inspection for ascus formation, a sample of each culture was resuspended in 100 µl of sterile water, and 4 µl of Zymolyase 100T (10 mg/ml) was added, followed by incubation for 7–10 min at room temperature. A 15 µl volume of the suspension was streaked out on to a YEPD plate and spores were segregated using a Singer MSM400 micromanipulator (Singer Instruments, Roadwater, Somerset, UK). Plates were incubated for 3 days at 30°C, and colony formation was documented by scanning and image processing as described for the serial drop-dilution assays.

For manipulations in *E. coli*, strain DH5α was employed with standard media as described previously (Straede and Heinisch, 2007).

### Construction of plasmids, deletion mutants and gene tagging

Wild-type genes from *K. lactis* were obtained by PCR using appropriate oligonucleotides with restriction sites and genomic DNA of strain CBS2359 or its derivatives as templates. Clones were verified by sequencing to contain no errors leading to amino acid exchanges in the protein coding regions. All vectors and plasmids employed are listed in Table S2. In the case of *KIDCK1*, PCR cloning was combined with gap repair analogous to the procedure described for *S. cerevisiae* (Oldenburg et al., 1997), since because of the large open reading frame of *KIDCK1* (5823 bp), all primary

clones constructed contained PCR errors in the protein coding sequence. Therefore, the wild-type sequence was regenerated by gap repair. Briefly, one of the plasmids with an erroneous PCR insertion was used to excise an internal fragment, dephosphorylated and introduced into a *K. lactis* recipient strain with a wild-type genomic *KIDCK1* allele. Sequencing of a recombinant clone isolated from such a transformant (pJH1409) confirmed that it carried the correct *KIDCK1* coding region.

Deletion strains were obtained by one-step gene replacement techniques described for *S. cerevisiae* (Rothstein, 1991), either by employing PCR products with 45–50 bp of flanking sequences homologous to the target gene, or by first creating longer flanking regions by *in vivo* recombination of the PCR products with the respective plasmids in *S. cerevisiae*, subcloning in pUK1921 (Heinisch, 1993) or its derivatives, and transformation of *K. lactis* after excision with restriction endonucleases or PCR amplification, as described previously (Heinisch et al., 2010). The recipient strain was either diploid and homozygous for the *ku80* deletion or haploid and also carrying this deletion to facilitate homologous recombination (Zonneveld and Steensma, 2003). Target gene deletions were obtained with either the *kanMX* or the *SkHIS3* cassette from the Longtine collection (Longtine et al., 1998), *SpHIS5* from pUG27 (Gueldener et al., 2002), or *ScLEU2* cassettes described previously (Heinisch et al., 2010). In the majority of cases, the *ku80* deletion was later eliminated by crossing with suitable *KU80* wild-type strains and tetrad analysis to avoid genomic instability. Fluorescence markers were derived from 3x mCherry and 3x myEGFP vectors described in Maeder et al. (2007), but carrying single fluorescence tags in the Longtine vector backbones (Table S2).

The mutant allele *KIRHO5*<sup>Q69H</sup>, which corresponds to the activated allele of *ScRHO5*<sup>Q91H</sup> described by Schmitz et al. (2002a), was obtained by string DNA synthesis from GeneArt (ThermoFisher Scientific) as a fragment containing the mutation and substituted for the respective wild-type sequence in a *KIRHO5* clone via homologous recombination in yeast. Similarly, a DNA fragment carrying the activated *KICDC42*<sup>G12V</sup> allele was obtained by string DNA synthesis and cloned into a vector carrying the wild-type allele.

A LifeAct probe with GFP as a fluorescent marker to follow actin dynamics *in vivo* was previously constructed for use in *K. lactis*, given that neither rhodamine phalloidin nor the commonly used LifeAct probe for *S. cerevisiae* worked in this yeast, probably because of a slightly different actin composition (Rippert et al., 2014). For colocalizations with GFP-KIRho5, the fluorophore was replaced by mRuby using homologous recombination and combined in an integrative plasmid with the tagged *RHO5* allele. KIMyo1-mCherry constructs have also been described previously (Rippert et al., 2014).

### Fluorescence microscopy

The setup used for fluorescence microscopy consisted of a Zeiss Axioplan 2 microscope (Carl Zeiss, Jena, Germany) equipped with a 100× alpha-Plan Fluor objective (numerical aperture 1.45) and differential interference contrast. Sample handling and image processing have been described in detail previously (Schmitz et al., 2015). Vacuoles were stained with 7-amino-4-chloromethylcoumarin (CMAC) as follows. A 1 ml sample of yeast cells grown to an OD<sub>600</sub> of 1.0 in synthetic medium was collected by centrifugation (10,000 g for 1 min at room temperature) and resuspended in 100 µl of fresh medium. An 8 µl volume of a 10 mM CMAC stock solution was added, and cells were incubated

for 1 h, washed with 1 ml of fresh medium and used for microscopic inspection. Colocalization was quantified by determining the Pearson coefficient, using the colocalize function of the FIJI/ImageJ program.

### Transmission electron microscopy

Yeast cells were grown to logarithmic phase in YEPD with shaking at 30°C and subjected to TEM as described in detail previously (Backhaus et al., 2010). In brief, cells were fixed with glutaraldehyde and potassium permanganate. After dehydration with ethanol and acetone, cells were suspended in Epon 812 for polymerization. To obtain 70 nm thick sections, a Leica Ultracut UC7 ultramicrotome was employed, and, after staining with uranyl acetate and lead citrate, samples were examined using a Zeiss TEM902A electron microscope at 80 kV.

### Acknowledgements

We are grateful to Hans-Peter Schmitz for invaluable advice on fluorescence microscopy and statistical analyses. We also thank Andrea Murra for excellent technical assistance and Rosaura Rodicio for critical reading of the manuscript.

### Competing interests

The authors declare no competing or financial interests.

### Author contributions

Conceptualization: J.J.H.; Methodology: C.C.S., C.M.; Software: M.M., J.J.H.; Validation: A.P., J.J.H.; Formal analysis: M.M., J.J.H.; Investigation: M.M., C.C.S., F.S., C.M., J.J.H.; Resources: J.J.H.; Writing - original draft: J.J.H.; Writing - review & editing: M.M., C.C.S., F.S., C.M., A.P., J.J.H.; Visualization: M.M., C.M.; Supervision: A.P., J.J.H.; Project administration: J.J.H.; Funding acquisition: J.J.H.

### Funding

This work was funded by a grant from the Deutsche Forschungsgemeinschaft (DFG; HE 1880/6-1).

### Peer review history

The peer review history is available online at <https://journals.biologists.com/jcs/article-lookup/doi/10.1242/jcs.258301>.

### References

- Andrejc, D., Možir, A. and Legiša, M. (2017). Effect of the cancer specific shorter form of human 6-phosphofructo-1-kinase on the metabolism of the yeast *Saccharomyces cerevisiae*. *BMC Biotechnol.* **17**, 41. doi:10.1186/s12896-017-0362-5
- Annan, R. B., Wu, C., Waller, D. D., Whiteway, M. and Thomas, D. Y. (2008). Rho5p is involved in mediating the osmotic stress response in *Saccharomyces cerevisiae*, and its activity is regulated via Msi1p and Npr1p by phosphorylation and ubiquitination. *Eukaryot. Cell* **7**, 1441-1449. doi:10.1128/EC.00120-08
- Backhaus, K., Heilmann, C. J., Sorgo, A. G., Purschke, G., de Koster, C. G., Klis, F. M. and Heinisch, J. J. (2010). A systematic study of the cell wall composition of *Kluyveromyces lactis*. *Yeast* **27**, 647-660. doi:10.1002/yea.1781
- Barsoum, E., Rajaei, N. and Åström, S. U. (2011). RAS/cyclic AMP and transcription factor Msn2 regulate mating and mating-type switching in the yeast *Kluyveromyces lactis*. *Eukaryot. Cell* **10**, 1545-1552. doi:10.1128/EC.05158-11
- Cao, L., Tang, Y., Quan, Z., Zhang, Z., Oliver, S. G. and Zhang, N. (2016). Chronological lifespan in yeast is dependent on the accumulation of storage carbohydrates mediated by Yak1, Mck1 and Rim15 kinases. *PLoS Genet.* **12**, e1006458. doi:10.1371/journal.pgen.1006458
- Coria, R., Kawasaki, L., Torres-Quiroz, F., Ongay-Larios, L., Sanchez-Paredes, E., Velazquez-Zavala, N., Navarro-Olmos, R., Rodriguez-Gonzalez, M., Aguilar-Corachan, R. and Coello, G. (2006). The pheromone response pathway of *Kluyveromyces lactis*. *FEMS Yeast Res.* **6**, 336-344. doi:10.1111/j.1567-1364.2005.00022.x
- Eliš, M. and Klimeš, V. (2012). Rho GTPases: deciphering the evolutionary history of a complex protein family. *Methods Mol. Biol.* **827**, 13-34. doi:10.1007/978-1-61779-442-1\_2
- Gueldener, U., Heck, S., Fielder, T., Beinhauer, J. and Hegemann, J. H. (1996). A new efficient gene disruption cassette for repeated use in budding yeast. *Nucleic Acids Res.* **24**, 2519-2524. doi:10.1093/nar/24.13.2519
- Gueldener, U., Heinisch, J., Koehler, G. J., Voss, D. and Hegemann, J. H. (2002). A second set of *loxP* marker cassettes for Cre-mediated multiple gene knockouts in budding yeast. *Nucleic Acids Res.* **30**, e23. doi:10.1093/nar/30.6.e23
- Heinisch, J. J. (1993). *PFK2, ISP42, ERG2* and *RAD14* are located on the right arm of chromosome XIII. *Yeast* **9**, 1103-1105. doi:10.1002/yea.320091010
- Heinisch, J. J. and Brandt, R. (2016). Signaling pathways and posttranslational modifications of tau in Alzheimer's disease: the humanization of yeast cells. *Microb. Cell* **3**, 135-146. doi:10.15698/mic2016.04.489
- Heinisch, J. J., Buchwald, U., Gottschlich, A., Heppeler, N. and Rodicio, R. (2010). A tool kit for molecular genetics of *Kluyveromyces lactis* comprising a congenic strain series and a set of versatile vectors. *FEMS Yeast Res.* **10**, 333-342. doi:10.1111/j.1567-1364.2009.00604.x
- Hühn, J., Musielak, M., Schmitz, H.-P. and Heinisch, J. J. (2019). Fungal homologues of human Rac1 as emerging players in signal transduction and morphogenesis. *Int. Microbiol.* **23**, 43-53. doi:10.1007/s10123-019-00077-1
- Kumar, A., Dandekar, J. U. and Bhat, P. J. (2017). Fermentative metabolism impedes p53-dependent apoptosis in a Crabtree-positive but not in Crabtree-negative yeast. *J. Biosci.* **42**, 585-601. doi:10.1007/s12038-017-9717-2
- Lam, B. D. and Hordijk, P. L. (2013). The Rac1 hypervariable region in targeting and signaling: a tail of many stories. *Small GTPases* **4**, 78-89. doi:10.4161/sstp.23310
- Lamas-Maceiras, M., Rodríguez-Belmonte, E., Becerra, M., González-Siso, M. I. and Cerdán, M. E. (2015). KIGcr1 controls glucose-6-phosphate dehydrogenase activity and responses to H<sub>2</sub>O<sub>2</sub>, cadmium and arsenate in *Kluyveromyces lactis*. *Fungal Genet. Biol.* **82**, 95-103. doi:10.1016/j.fgb.2015.07.004
- Lippincott, J. and Li, R. (1998). Sequential assembly of myosin II, an IQGAP-like protein, and filamentous actin to a ring structure involved in budding yeast cytokinesis. *J. Cell Biol.* **140**, 355-366. doi:10.1083/jcb.140.2.355
- Llacer, J. L., Hussain, T., Saini, A. K., Nanda, J. S., Kaur, S., Gordiyenko, Y., Kumar, R., Hinnebusch, A. G., Lorsch, J. R. and Ramakrishnan, V. (2018). Translational initiation factor eIF5 replaces eIF1 on the 40S ribosomal subunit to promote start-codon recognition. *eLife* **7**, e39273. doi:10.7554/eLife.39273
- Longtine, M. S., McKenzie, A., III, Demarini, D. J., Shah, N. G., Wach, A., Brachat, A., Philippsen, P. and Pringle, J. R. (1998). Additional modules for versatile and economical PCR-based gene deletion and modification in *Saccharomyces cerevisiae*. *Yeast* **14**, 953-961. doi:10.1002/(SICI)1097-0061(199807)14:10<953::AID-YEA293>3.0.CO;2-U
- Lorberg, A., Schmitz, H. P., Gengenbacher, U. and Heinisch, J. J. (2003). *KIROM2* encodes an essential GEF homologue in *Kluyveromyces lactis*. *Yeast* **20**, 611-624. doi:10.1002/yea.989
- Maeder, C. I., Hink, M. A., Kinkhabwala, A., Mayr, R., Bastiaens, P. I. H. and Knop, M. (2007). Spatial regulation of Fus3 MAP kinase activity through a reaction-diffusion mechanism in yeast pheromone signalling. *Nat. Cell Biol.* **9**, 1319-1326. doi:10.1038/ncb1652
- Mangione, M. C. and Gould, K. L. (2019). Molecular form and function of the cytokinetic ring. *J. Cell Sci.* **132**, jcs226928. doi:10.1242/jcs.226928
- Marei, H. and Malliri, A. (2017). Rac1 in human diseases: the therapeutic potential of targeting Rac1 signaling regulatory mechanisms. *Small GTPases* **8**, 139-163. doi:10.1080/21541248.2016.1211398
- Mehlgarten, C., Krijger, J. J., Lemnian, I., Gohr, A., Kasper, L., Diesing, A. K., Grosse, I. and Breunig, K. D. (2015). Divergent evolution of the transcriptional network controlled by Snf1-interacting protein Sip4 in budding yeasts. *PLoS ONE* **10**, e0139464. doi:10.1371/journal.pone.0139464
- Mojardin, L., Vega, M., Moreno, F., Schmitz, H.-P., Heinisch, J. J. and Rodicio, R. (2018). Lack of the NAD(+)-dependent glycerol 3-phosphate dehydrogenase impairs the function of transcription factors Sip4 and Cat8 required for ethanol utilization in *Kluyveromyces lactis*. *Fungal Genet. Biol.* **111**, 16-29. doi:10.1016/j.fgb.2017.11.006
- Nordmann, D., Lickfeld, M., Warnsmann, V., Wiechert, J., Jendretzki, A. and Schmitz, H.-P. (2014). The small GTP-binding proteins AgRho2 and AgRho5 regulate tip-branching, maintenance of the growth axis and actin-ring-integrity in the filamentous fungus *Ashbya gossypii*. *PLoS ONE* **9**, e106236. doi:10.1371/journal.pone.0106236
- Nouri, K., Timson, D. J. and Ahmadian, M. R. (2020). New model for the interaction of IQGAP1 with CDC42 and RAC1. *Small GTPases* **11**, 16-22. doi:10.1080/21541248.2017.1321169
- Oldenburg, K. R., Vo, K. T., Michaelis, S. and Paddon, C. (1997). Recombination-mediated PCR-directed plasmid construction in vivo in yeast. *Nucleic Acids Res.* **25**, 451-452. doi:10.1093/nar/25.2.451
- Ozdemir, E. S., Jang, H., Gursoy, A., Keskin, O., Li, Z., Sacks, D. B. and Nussinov, R. (2018). Unraveling the molecular mechanism of interactions of the Rho GTPases Cdc42 and Rac1 with the scaffolding protein IQGAP2. *J. Biol. Chem.* **293**, 3685-3699. doi:10.1074/jbc.RA117.001596
- Park, H.-O. and Bi, E. (2007). Central roles of small GTPases in the development of cell polarity in yeast and beyond. *Microbiol. Mol. Biol. Rev.* **71**, 48-96. doi:10.1128/MMBR.00028-06
- Rippert, D. and Heinisch, J. J. (2016). Investigation of the role of four mitotic septins and chitin synthase 2 for cytokinesis in *Kluyveromyces lactis*. *Fungal Genet. Biol.* **94**, 69-78. doi:10.1016/j.fgb.2016.07.007
- Rippert, D., Heppeler, N., Albermann, S., Schmitz, H.-P. and Heinisch, J. J. (2014). Regulation of cytokinesis in the milk yeast *Kluyveromyces lactis*. *Biochim. Biophys. Acta* **1843**, 2685-2697. doi:10.1016/j.bbamcr.2014.07.020

- Rodicio, R. and Heinisch, J. J. (2013). Yeast on the milky way: genetics, physiology and biotechnology of *Kluyveromyces lactis*. *Yeast* **30**, 165-177. doi:10.1002/yea.2954
- Rodicio, R., Koch, S., Schmitz, H. P. and Heinisch, J. J. (2006). *KIRHO1* and *KIPKC1* are essential for cell integrity signalling in *Kluyveromyces lactis*. *Microbiology (Read.)* **152**, 2635-2649. doi:10.1099/mic.0.29105-0
- Rodicio, R., López, M. L., Cuadrado, S., Cid, A. F., Redruello, B., Moreno, F., Heinisch, J. J., Hegewald, A.-K. and Breunig, K. D. (2008). Differential control of isocitrate lyase gene transcription by non-fermentable carbon sources in the milk yeast *Kluyveromyces lactis*. *FEBS Lett.* **582**, 549-557. doi:10.1016/j.febslet.2008.01.017
- Rose, M. D., Winston, F. and Hieter, P. (1990). *Methods in Yeast Genetics*. New York: Cold Spring Harbour Laboratory.
- Rothstein, R. (1991). Targeting, disruption, replacement, and allele rescue: integrative DNA transformation in yeast. *Methods Enzymol.* **194**, 281-301. doi:10.1016/0076-6879(91)94022-5
- Santomartino, R., Camponeschi, I., Polo, G., Immesi, A., Rinaldi, T., Mazzoni, C., Brambilla, L. and Bianchi, M. M. (2019). The hypoxic transcription factor KIMga2 mediates the response to oxidative stress and influences longevity in the yeast *Kluyveromyces lactis*. *FEMS Yeast Res.* **19**, foz020. doi:10.1093/femsyr/foz020
- Schmidt, M., Bowers, B., Varma, A., Roh, D.-H. and Cabib, E. (2002). In budding yeast, contraction of the actomyosin ring and formation of the primary septum at cytokinesis depend on each other. *J. Cell Sci.* **115**, 293-302. doi:10.1242/jcs.115.2.293
- Schmitz, H.-P., Huppert, S., Lorberg, A. and Heinisch, J. J. (2002a). Rho5p downregulates the yeast cell integrity pathway. *J. Cell Sci.* **115**, 3139-3148. doi:10.1242/jcs.115.15.3139
- Schmitz, H.-P., Lorberg, A. and Heinisch, J. J. (2002b). Regulation of yeast protein kinase C activity by interaction with the small GTPase Rho1p through its amino-terminal HR1 domain. *Mol. Microbiol.* **44**, 829-840. doi:10.1046/j.1365-2958.2002.02925.x
- Schmitz, H.-P., Jendretzki, A., Wittland, J., Wiechert, J. and Heinisch, J. J. (2015). Identification of Dck1 and Lmo1 as upstream regulators of the small GTPase Rho5 in *Saccharomyces cerevisiae*. *Mol. Microbiol.* **96**, 306-324. doi:10.1111/mmi.12937
- Schmitz, H. P., Jendretzki, A., Sterk, C. and Heinisch, J. J. (2018). The small yeast GTPase Rho5 and its dimeric GEF Dck1/Lmo1 respond to glucose starvation. *Int. J. Mol. Sci.* **19**, 2186. doi:10.3390/ijms19082186
- Singh, K., Kang, P. J. and Park, H.-O. (2008). The Rho5 GTPase is necessary for oxidant-induced cell death in budding yeast. *Proc. Natl. Acad. Sci. USA* **105**, 1522-1527. doi:10.1073/pnas.0707359105
- Singh, K., Lee, M. E., Entezari, M., Jung, C.-H., Kim, Y., Park, Y., Fioretti, J. D., Huh, W.-K., Park, H.-O. and Kang, P. J. (2019a). Genome-wide studies of Rho5-interacting proteins that are involved in oxidant-induced cell death in budding yeast. *G3 (Bethesda)* **9**, 921-931. doi:10.1534/g3.118.200887
- Singh, V., Davidson, A. C., Hume, P. J., Humphreys, D. and Koronakis, V. (2019b). Arf GTPase interplay with Rho GTPases in regulation of the actin cytoskeleton. *Small GTPases* **10**, 411-418. doi:10.1080/21541248.2017.1329691
- Sterk, C., Graber, L., Schmitz, H. P. and Heinisch, J. J. (2019). Analysis of functional domains in Rho5, the yeast homolog of human Rac1 GTPase, in oxidative stress response. *Int. J. Mol. Sci.* **20**, 5550. doi:10.3390/ijms20225550
- Straede, A. and Heinisch, J. J. (2007). Functional analyses of the extra- and intracellular domains of the yeast cell wall integrity sensors Mid2 and Wsc1. *FEBS Lett.* **581**, 4495-4500. doi:10.1016/j.febslet.2007.08.027
- Takai, Y., Sasaki, T. and Matozaki, T. (2001). Small GTP-binding proteins. *Physiol. Rev.* **81**, 153-208. doi:10.1152/physrev.2001.81.1.153
- Williams, C. L. (2003). The polybasic region of Ras and Rho family small GTPases: a regulator of protein interactions and membrane association and a site of nuclear localization signal sequences. *Cell. Signal.* **15**, 1071-1080. doi:10.1016/S0898-6568(03)00098-6
- Woods, B. and Lew, D. J. (2019). Polarity establishment by Cdc42: Key roles for positive feedback and differential mobility. *Small GTPases* **10**, 130-137. doi:10.1080/21541248.2016.1275370
- Zonneveld, B. and Steensma, H. (2003). Mating, sporulation and tetrad analysis in *Kluyveromyces lactis*. In *Non-Conventional Yeasts in Genetics, Biochemistry and Biotechnology* (ed. K. Wolf, K. D. Breunig and G. Barth), pp. 151-154. Berlin: Springer Verlag.

# Rho5

switch I

switch II

```
KlRho5p : MRSIKCVVVGDAVGKTSLLISYTTNFFDYIPTVFDNYSTTIALED-----PYNPDSHQIIEKLNLDWDTAGOEYDRLRPLSYPTDFLFLIC : 89
ScRho5p : MRSIKCVIIGDGAVGKTSLLISYTTNFFDYVPTVFDNYSTTIAIPNGTASSPLELDNGDKRGLSSASSSPSTDRKLYKLNLDWDTAGOEYDRLRPLCYPTDFLFLIC : 111
HsRac1p : MQATKCVVVGDAVGKTCLLISYTTNAFFGEYIPTVFDNYSANVMVDG-----RPVNLGLWDTAGOEYDRLRPLSYPTDFLFLIC : 81

KlRho5p : FSVNEPNSFENVYDKWVPEIKHSTNFFENLDLYHQSKLPIILLVGTTRADLRDDHEHRLQESNSDQVSOQOIQELVNKLCIMGYVECSAATQVGVREVFBAVDCVVVEP : 199
ScRho5p : FSVSEHASFANVTEKWLPELKQTSNIEGTSLSYTKLCKYPIILLVGTTRADLRDDPATOKKIQEANSQVVSQOEIIDEVQRCGMGYVECSAATQAGVREVFEOAVRYAIVVEPE : 222
HsRac1p : FSLVSPASFENVRAKWPPEVRHHC-----P-NTPIILLVGTTRADLRDDKDIIEKIKKPKLTPFLTPYQGLAVAKEICAVKVECSALTQRGLKTVDEAIVRAVLCPP : 180

KlRho5p : -----DRLVRE-----SLQCKQQVQDSQ-----QKPKTKQVNNK-----NTTAQPESSTKPKQSKRSIKRKCITLI : 254
ScRho5p : SPNQSANHTLTDLTTATTNTNGDKNIRESQKQPHHNNSTDSTLPGKSLOQEKPLNLIKPTKKGQKDKIIEQSKSGSKIASNHNHKNQAKPKTRNDKKRKRKSKCVILL : 331
HsRac1p : -----P-----VKKRKRKCITLI : 192
```

**S. cerevisiae-specific extension**

**PBR-CAAX**

# Dck1

SH3 domain

```
KlDck1p : MTKSNNDATANGSSDTPANHELTRQFWMPTDRLIPCTVARAFDPKCKPELVLSKSDVVDLPEGDEVFVMEQTDKQKWCRCVSNLDLIDPEMNNCGSVTDNLEPKQIQRVIFPRRFVLDLDFEQIENYAGL : 133
ScDck1p : MSQQDSQR-----MPTDRLIPCTVARAFDPKCKPELVLSKSDVVDLPEGDEVFVMEQTDKQKWCRCVSNLDLIDPEMNNCGSVTDNLEPKQIQRVIFPRRFVLDLDFEQIENYAGL : 114

KlDck1p : RFTGTLEEQDGRLLKPLSYQLMRAISKVS-----RETF-PPVFFVANGYALNREILLNFTLTKELYVLYSFGEEIEVDQVLDLKYKLDVAVIQVQANFMATNDRSLIMKKAVALMSIFSSTIASHSV : 258
ScDck1p : KAFSAEDFKPLISKECESRSEFCDSLVSSTDDISTGPKPKTRPPPEFFRYQKRSFKDEMGPISLISSEVYSMSYSGEESHYRKKIKLAVYDQDITIFRSMNLTTEAKINLIRAATSURTAKIAGLSSSYR : 247

KlDck1p : TRKIGSLQKRRNIDEGFSESLTRDQATCKLLTDSVS-PQLMATSSTVYAMTNTVSVSNANDLKLKPDENTRKKSFPFSCITVDCQEIIG-TLVSDQHAEAHTAYLYLRTAKEVLTPELIDLKRNQKSMQN : 389
ScDck1p : KNKLIANSTRPNPDEYGFEGCFARDIDTCELLSYEIDKLRTLVSSMCGLNNFTVPVVSSDDESSSGLGCVVR-SLILVNKLDAWDPSTSDPKYQDLSICVYLRTKDEVLTSESMTKSSNMESALDE : 379

KlDck1p : VSALEFRNLFPYNGENRNVVLVVEIVETIKVVIDED-----VDQKFKVPEVFAASADDITGSIIRRCVVAGATDTSRVTSKEKSLASGHAVNKEVLFASFYTDKSEQPPIPAATLTDPAKLAKLM : 512
ScDck1p : IEMLEFRNILETIHVKKVVILVVLKETTMAITTEAPEISSYNISTESSHSESPSSNSTENKIDHVKKGLACGVINISVREKFNGLSVANKAQRANLYLVSQSSDSQN----- : 492

KlDck1p : KAKSNVSTKNGWGDIDRINDSHTCIAVGTQMESLVSVKEIKEDCKFLQTNSDNAMAHTAVNPIFYDTLEQKQTDRIYLTDRKVSICGLENKKSNVSNHTHOISSNNDKITERPSSVTHSYKKAETITVR : 645
ScDck1p : --FNSSKADLWGCGLNKTIKDSSECVSNPRAVSLSVVKEIIGKQEAQKVLSTSLVPRSIPTVYDTMFS-CAERIVYINLGRVSLYCPAADNINENVTVQISCRNKAVKCKKNLEERSGDVWKEVSVR : 622

KlDck1p : PGLVNEHTIADGIDSYTKETLRVSAYLNGRIFAKSRYVKKGLQELYEYKSKSVOLISSLCKPVEIEVGTREVNNTNMDRTHVSHISLRLRHQITENDFEQSLKALSKRMVSHKQITRYENPHTLSI : 778
ScDck1p : PMSIGESIRIPEGVENNEDETLRVLVYLNCFWAKSNHILKKNETIEYRKGVEQIMSSKSVPLIHLLEASFFERRNINPAITNPLVQTNVVEFDQQLKEHYSVTLKQNNVSEFKOLLKHEDTLTAHY : 755

KlDck1p : ILELYYTCYRHAAR-SEEAQKKAQVFSLVQFTDMNIAHRDNYKHLNDFEEVRENSNYLPELQETVRLVSECFSSANSWSVYRALCF--SYLLKIKLRLFSKDIVGYHQAVDEFFNSLSIFRVTND : 908
ScDck1p : LLTESVNEATDKKGFSSSNLIVFESHFKFNLMTHQENSRVWNRLYKQMS-KELEENVAETIKHMTIERSHSSWTTATACRCTLILYIVLALCSSHSDDEMP---NFSHFERSHKSLMLADE : 883

KlDck1p : SVLVDQVITILETYDLAINETSADFDDPHITQLVLLFNACQEKENSIEFSQDDISSTKNEFNARVLLRRLIQNPDAFFFK-DPAENPLTKRSLQVIEWCFKFEIKEKGCVPNLTASYANGLVITITTEQ : 1040
ScDck1p : PIMADQILLIESIPSMLEMTNHCQVEDVVRFAIGLRECCQEKEMNKMYSRPISVREBEYLNTKFNCLIKLINKKVVQNYLNTNTEVDKLRLOLTKSTLEWLLTETVPGDDCKCFHVESLRLVNSVFTITTEQ : 1016

KlDck1p : AQDTVFRNLIRLLEIFCRILELRSACQEKEDCFKRVFALEFETVTELPETIIVDSVVDDEVFVQVILETMTITIALTKIVEQQYDSHGSEIKAKAEAREDEEOSPYVTKIVREDLAITEVTHRLIKGQ : 1173
ScDck1p : YKFDMLQNLIRLLEYLCKSEVHARRYCKKARLMRPRVFMLEPEREICNYIIPVDSIVNDEVFVQVILELITCETITKASSRFSYQSSSEIINLQDKTLEQSNFVSRQITNENVYATPKVFLFFEQD : 1149

KlDck1p : FFEKRWPTMRAIMRACMTISEMCLDVFKLYYVD-EQCTLETFABWGRVFRVLCIANHKTVNSFPLAPLPRKAVYLVGDLIGRASYTEEQITWITLGDNCIGTDLDNKYCLRRSVYQMTFLTAAMD : 1305
ScDck1p : WFGMKGVLGVSALLGSSLLPLSLCKDYIENNSESPKSEKRVDMRWAEEVVRVILVSNKESASIKLALITPRKAVYLVGDLIKKISAYITNECWDAPATGHYNTYAKKYGALSDCCFELFVHQFL : 1282

KlDck1p : VTDCAQSELRVDAFVGSKIIVVLILVWNNENSTIAIEELTQOPENAYQKALRPVVEVEIADITLHVILHLDTDSIKDTLFNYYRFKPEPLSLAETEDPSCFEFDDRTASQIRICVYLSMKR : 1438
ScDck1p : IREIFIAERHIDRTRICKKILGGLNFRIRIFGSLQFPVNAICPELESAYQICKLNDYELERVSCFFMHWVPSDSTFFPACMDELDDLGPHIVNEIYKIPNCEFFDDRTARHIEVBYLLEANA : 1415

KlDck1p : PEMLETLVNDLFINHMRRKDYIQAAALSLELLALTYEWNENDSIPATKVPPLPEQSSFEREYIKBARNFNPKGKURKALVYKIDADAYDKINVDLGLSYVHGOISNITYTDLQNDRLVENVYKVSVEYCY : 1571
ScDck1p : PELFEKMIVDLFIHFOKQDFVQAAALSLELLACTYANDSNDLSEIPPLPEQSSFEREYIKESARNSFCQKPKKALAVYKIDKAYDEINVDLNGAFVHDOAGTYTRELQSDRLVPTFYKVSVMCF : 1548

KlDck1p : GFFKMLEGKTEVPEGLPFPHITSEHRLIKLIPCKLUNSTPEADKLVVSPFKGKTHVIVSVEERFOLESDYATSDKKN-DNNKVRLYVENRDLKTFSSRRVAGTHGTDLWVIEYIIEFKSFFPTLMNRSE : 1703
ScDck1p : GFFKSLNKSSEVPEGLPFPHITSEHRLIKLIPCKLUNSTPEADKLVVSPFKGKTHVIVSVEERFOLESDYATSDKKN-DNNKVRLYVENRDLKTFSSRRVAGTHGTDLWVIEYIIEFKSFFPTLMNRSE : 1681

KlDck1p : VVKVTEKRLSPINNAIKSLQKIQEISGLEDKCYKLMKENDCSEVSELSRNITGTTDAFNGGIAEVRVETDEETSKLDPADVELVAAANEITIVNRCIALHGCQCE-ISLKSSETLLKDLAKNBE : 1835
ScDck1p : IVKVTKSLSELENARSLOVQIQEIVGLENMCKNLTQKHDVNDLFEIENITGTTDAFVNGGISQKAELEPSTSK-QFSTDGLGRITLADDEIVAVICRQITFAEILESKDKESHTVVRVSEENFA : 1813

KlDck1p : KETIKVSGIDINETN---DETHARKSIQSSQQSFKRSSMLMRSIFSESHRSISAGSNGSATKNSMHDIVVSESHRTKSNAP---SHAAASHATRISREPTTHISMRLRSTR----- : 1940
ScDck1p : EETERYSRITSEANRSRNNMTHARTIISHKNPKKASFSGRDHTTSGSNHSQVLEHSDSPFNSSLFGKYLITLISSTISLSDKSGIVSCTSTFLAGSCFNNTDSQHKKDYSHSG : 1932
```

**DHR1 and DHR2 domains**

# Lmo1

```
KlLmo1p : METIHDHNMHNKVDNHDGVMLQDIAEKYVIVVIAAFSQQSETDEALITLGLHLSLFAATDLWKP---RITDELISRLYGLITSTQSKDITLHASLSVLTLLENVVLHPPSSQISLTVLCSVLHSGPDILE : 131
ScLmo1p : MKHNRPMPDESLENIKVLLNPKLGKPVNSLTSQAQRACYHFLISNKNKNTSDEYERLQNYLILLCDKEYLCKTVIPDSRFWALLCDNQCQIRSETLVANLIRIFNVALKCQDSNKNEVIVSICHISRENSOLIG : 135

KlLmo1p : QFVCLLKYENNPTTQGEIKYLCQHVICHQWVSEGDKTAVTEVARTNMMEDVGVNLNLSCLLYAHEHNKDLVSGIISQELVQLRPLKGAVKDLPNNEVLEATDVVKBILHKLFDVYEITQERFKSNEEYTD : 266
ScLmo1p : ILLQQLSQRPPIHILPFTDITLCTIFLKSITLTCETSLSHAVEVPRILLILFQYNFPASMSSELYLIEDLQPLIL---EEVPLKQINFLNLSVSIIDY---SCSLKADLITALKDNSVFQKGLVEMG---D : 260

KlLmo1p : LGLIVQOLLNIRFITRONDLFEKAWTEOIMFEYPLDILKTVARLSVIVVDYVEMSNLKLG-----SFKVHMHFIFFTKEIIVAVLQTMVTLDKSRSETEDPESELPELTKLILH----KADKICRTR : 388
ScLmo1p : LPSINLQNAIDTFTFINSPNGSFRRLVTEQLLEGNDFEYEAIFKLSQQFRRLLENLGRKENQYSDSERDILQIATAVLNRQTCFYKTELEFLRFVLESKAKSOSLVSLINLAIITLKYVCLSSSDLEAAIQ : 395

KlLmo1p : HDSFVEHFEVCEFTTDEDLQVAEWREKQFNDWAEITSSFEELQNVQDFVRYQRLLMOKGTWVYSNPELEAKDKIPKVSLEALSQVQMLLIKEKHKVKEKTPVVDNCHVVIDHS-AMVNNKQIVHPI : 522
ScLmo1p : TRSLKIQVVALDSMRKCFARLQDSIKKCYRTSSSTASFDTMSGQVRVYVRRQRLIQKGTWVYAGNEINPEAGTEPKYKVIIVSDNHANLAREBETQNTNDLYFLDNKILSPGSBALAGRQKVVVI : 530

KlLmo1p : KNINICRQIELDKRLPEGVRLINILQNTIYREVTTFDRNGKILSAFYLESSEFVWLDGLQELFOSKFAKISPEPEKQIDVYLKLRNVQALALDDKFRDDESLESESEBETDFFVYNPELTKQLSMGLIYVE : 657
ScLmo1p : RHTSFRSIELTTPSRRTSSNVYIKLDEANVYTCVELKDRNDRTVLRKFTYDTEGRVYWLDGLQELFOSKFAKISPEPEKQIDVYLKLRNVQALALDDKFRDDESLESESEBETDFFVYNPELTKQLSMGLIYVE : 665
```

**PH domain**

**EAD domain**

**ELMO domain**

**Fig. S1. DLR components of *K. lactis* are conserved in their functional domains with their homologs in *S. cerevisiae*.** Identical amino acid residues are highlighted by inverse print, conserved amino acid residues by light gray background. Upper rows: The deduced amino acid sequence of KIRho5 was aligned both to ScRho5 and human Rac1 (HsRac1p). Highly conserved functional domains (switch I, switch II, PBR, and CAAX-box) are indicated by boxes. Of special interest, ScRho5 carries a specific extension not present in HsRac1 and drastically shorter in KIRho5, also marked by a box. Middle rows: Alignment of the homologs of the GEF subunit Dck1 from *K. lactis* and *S. cerevisiae*. Functional domains described for ScDck1 are indicated. Lower rows: Alignment of the homologs of the GEF subunit Lmo1 from *K. lactis* and *S. cerevisiae*. Described functional domains are boxed and designated.

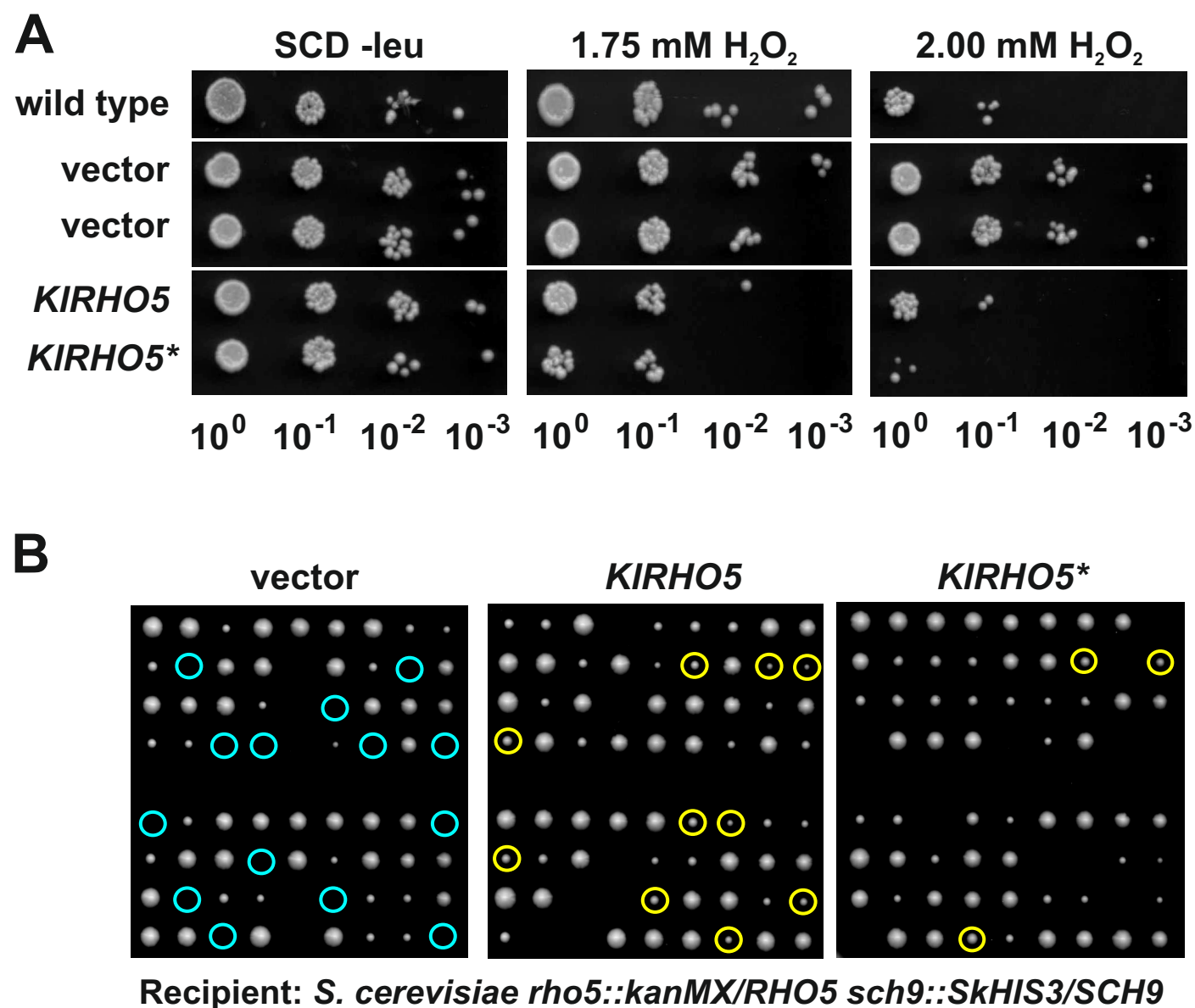


**Fig. S2. *Scrho5* deletion phenotypes are complemented by its homolog *KIRHO5***

A) Drop-dilution assays of HOD342-6D carrying the vector without insertion (vector = YEp181JJH), the same vector with the wild-type allele of the *K. lactis* homolog (*KIRHO5* = pJJH2759), and its activated allele (*KIRHO5\** = *KIRHO5*<sup>Q69H</sup> = pJJH2760). As a control, the *ScRHO5* wild-type strain HD56-5A was transformed with the vector YEp181JJH and treated in the same way (upper lane). Ten-fold dilutions of logarithmically growing cultures were spotted onto plates lacking leucine with the concentrations of hydrogen peroxide as indicated as described in materials and methods. Growth was monitored by scanning after incubation at 30°C for 3 days.

B) The diploid strain DAJ138 with the heterozygous deletions indicated was used to introduce either the vector (YCplac111), or plasmids carrying the wild-type *KIRHO5* (pJJH2759) and the activated *KIRHO5\** (pJJH2760) allele of *K. lactis*. Transformants selected on synthetic medium lacking leucine were sporulated, subjected to tetrad analyses and replica-plated onto drop-out media for detection of the deletion markers and the presence of the plasmid. Blue circles indicate the position of segregants that should carry the *rho5 sch9* double deletion, but are synthetically lethal, yellow circles designate segregants carrying the double deletion and the plasmid with the respective *KIRHO5* allele. Note that *sch9* deletions form smaller colonies, independent of the *RHO5* allele they carry.

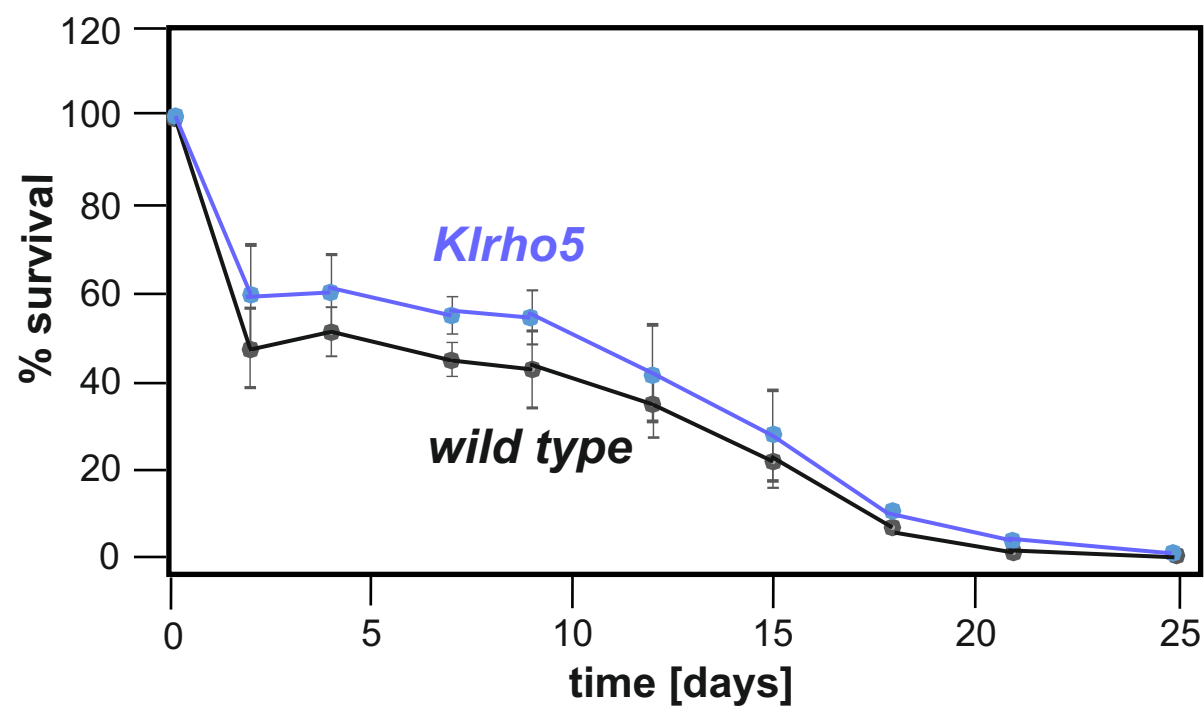


**Fig. S3. Deletion of *KIRHO5* does not affect chronological life span.** Two cultures of three independent strains, each being either wild-type for *KIRHO5* or carrying a deleted allele, were grown to stationary phase in synthetic selective medium (strains employed: wild-types KHO46-2A, KHO46-6C, KHO46-12B; *Klrho5* deletions KHO208-8B, KHO276-2A, KHO368-3B). Samples were taken at the time points indicated, diluted to produce single colonies, plated on rich medium (YEED) and incubated for three days to determine the number of colony-forming units (CFU). CFUs were set at 100% at day 0, with starting at approximately  $2 \times 10^7$  viable cells/mL. Error bars give the standard deviations of % survivors in the three biological replicates.

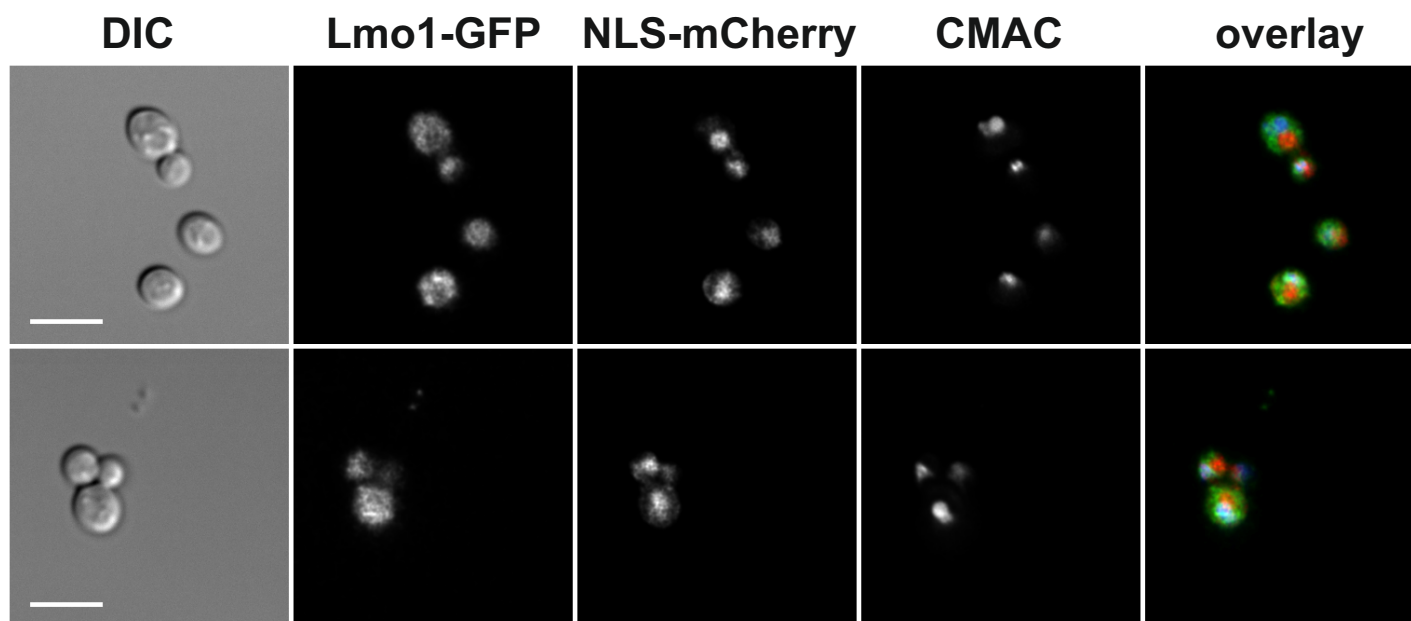
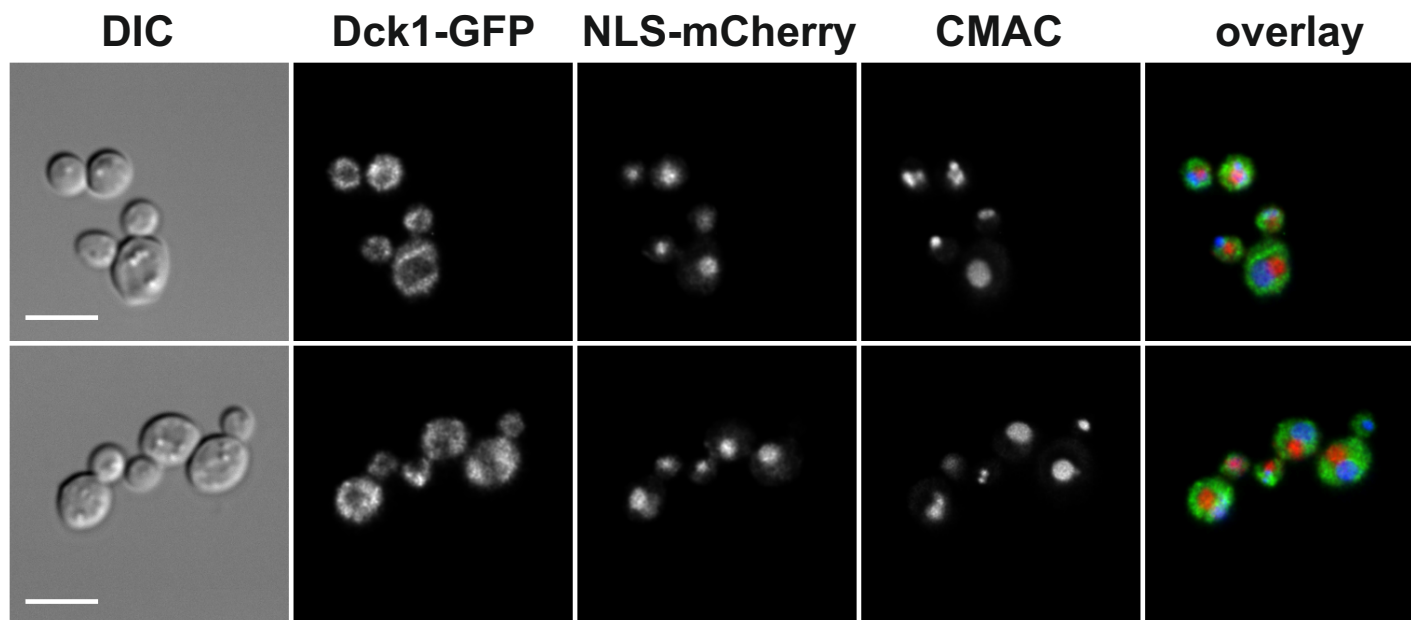


**Fig. S4. KIDck1-GFP and KILmo1-GFP do not strongly associate with the nucleus or vacuoles under standard growth conditions.** Strains carrying either the *KIDCK1-GFP* allele or the *KILMO1-GFP* allele at their native loci were crossed to a strain encoding a nuclear localization signal fused to mCherry integrated at the *Klleu2* locus, sporulated and subjected to tetrad analyses. Segregants expressing both fluorophore fusions were used for life-cell imaging. Vacuoles were stained with CMAC as described in materials and methods. Images were acquired with 0.5 sec exposures in the respective channels. The size bar in the lower left corner of the DIC images represents 5  $\mu\text{m}$ , applicable to all images in the panels of the same row.



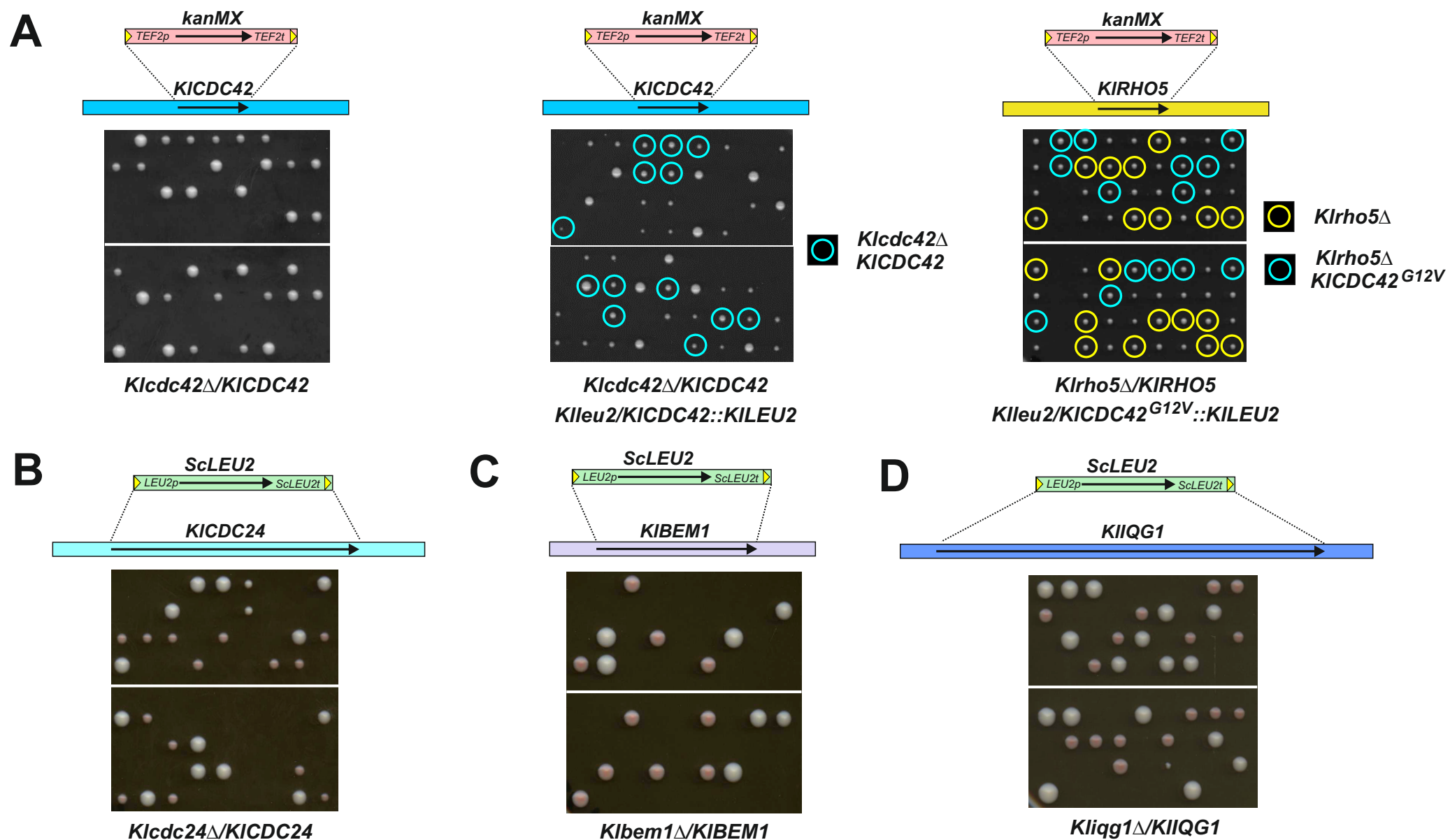


**Fig. S5. *KICDC42*, *KICDC24*, *KIBEM1*, and *KIIQG1* are essential genes.** Heterozygous diploids were constructed in the background of strain KHO70 by homologous recombination as indicated by the schematic representations, and subjected to tetrad analyses. Asci were dissected and allowed to germinate on YEPD plates, with 3-4 days incubation at 30°C. Relevant genotypes are indicated below the images (strains with complete genotypes are listed in Table S1). A) Tetrad analyses of strains carrying different *KICDC42* alleles. The original heterozygous diploid strain KHO70/*cdc42* did not yield viable progeny carrying the deletion marker (left). Integration of a wild-type copy at the *Klleu2* locus in this strain (pJJH2918) restored viability to segregants also carrying the deletion (middle, blue circles). No synthetic growth phenotypes were observed if combining the integrated activated *KICDC42<sup>G12V</sup>* allele (pJJH2917) with a *Klrho5* deletion (right, blue circles) as compared to the single *Klrho5* deletion (right, yellow circles). However, morphological defects of the deletion were compensated by the presence of the activated *KICDC42<sup>G12V</sup>* allele (see main text for details). B) to D) Segregants of heterozygous diploid strains carrying deletions of either *KICDC24*, *KIBEM1*, or *KIIQG1* were not viable, while auxotrophic markers in the viable wild-type colonies segregated as expected (exemplified by the red colony colour caused by a *Klade2* deletion in approximately half of the segregants).

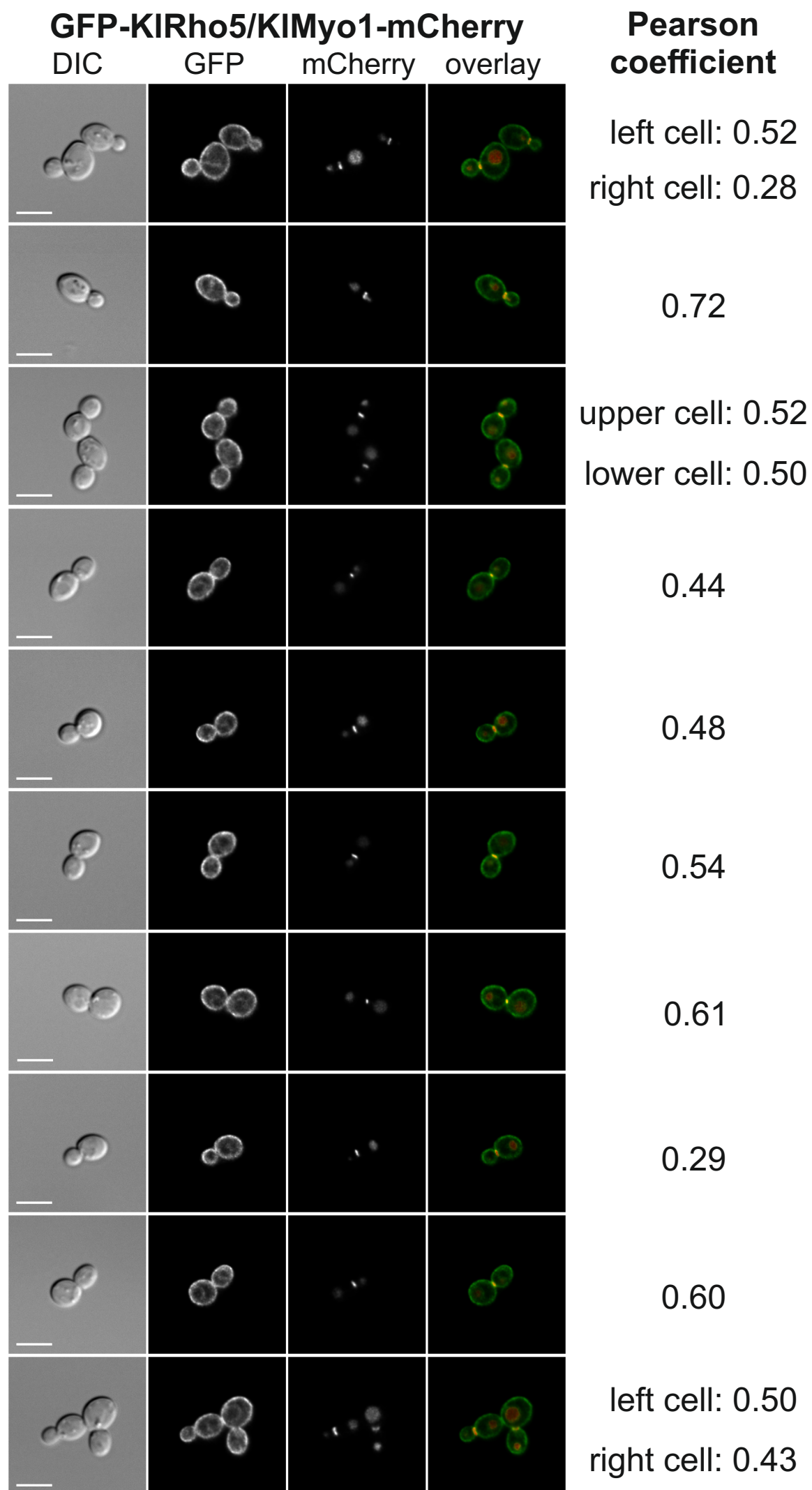


**Fig. S6.** Additional images showing the colocalization of GFP-KIRho5 and Myo1-mCherry at the bud neck of dividing cells. Strains, growth conditions, image acquisition and calculations of the Pearson coefficient were as described in the legend of Fig. 7.

**Table S1. Strains used in this study**

Strain	Collection number	Genotype	Reference
<b><i>Kluyveromyces lactis</i> strains <sup>1</sup></b>			
CBS2359	Os83	<i>MATa</i>	(Kooistra et al., 2004)
KHO70	- <sup>2</sup>	<i>MATa/MATalpha ura3/ura3 leu2/leu2 his3::loxP/HIS3 ade2::loxP/ADE2 ku80::loxP/ku80::loxP</i>	(Heinisch et al., 2010)
KHO70/bem1	K11250	same as KHO70 but with <i>bem1::ScLEU2/BEM1</i>	this study
KHO70/cdc24	K11245	same as KHO70 but with <i>cdc24::ScLEU2/CDC24</i>	this study
KHO70/cdc42	K11262	same as KHO70 but with <i>cdc42::ScLEU2/CDC42</i>	this study
KHO70/iqg1	K1482	same as KHO70 but with <i>iqg1::ScLEU2/IQG1</i>	this study
KHO.01-14C	K1642	<i>MATalpha dck1::kanMX</i>	this study
KHO.03-1D	K1644	<i>MATalpha lmo1::kanMX</i>	this study
KHO208-8A	K1390	<i>MATalpha ura3 leu2 his3::loxP ku80::loxP</i>	this study
KHO208-8B	K1391	<i>MATalpha ura3 leu2 his3::loxP rho5::kanMX ku80::loxP</i>	this study
KHO218-9A	K1428	<i>MATa ura3 leu2 his3::loxP dck1::kanMX</i>	this study
KHO254-1A	K11312	<i>MATalpha ura3 leu2 Kldck1::kanMX</i>	this study
KHO255-1B	K1648	<i>MATalpha ura3 leu2 Kllmo1::kanMX ku80::loxP</i>	this study
KHO255-3A	K1649	<i>MATalpha ura3 leu2 his3::loxP Kllmo1::kanMX ku80::loxP</i>	this study
KHO276-2A	K1652	<i>MATa ura3 his3::loxP rho5::kanMX</i>	this study
KHO277-3D	K1667	<i>MATalpha ura3 leu2 Klrho5::kanMX</i>	this study
KHO46-6C/2751	K11073	<i>MATa ura3 leu2::pJJH2751-LEU2</i>	this study

KHO347-2B	KI958	<i>MATa ura3 leu2 his3::loxP KU80wt DCK1-GFP-SkHIS3 IDP1-mRuby-kanMX</i>	this study
KHO348-2B	KI953	<i>MATa ura3 his3::loxP LMO1-GFP-SkHIS3 IDP1-mRuby-kanMX</i>	this study
KHO362	- <sup>2</sup>	<i>MATa/MATalpha ura3/ura3 leu2/leu2 his3::loxP/HIS3 ade2::loxP/ADE2 ku80::loxP/ku80::loxP Kllm1::kanMX/KILMO1</i>	this study
KHO364	- <sup>2</sup>	<i>MATa/MATalpha ura3/ura3 leu2/LEU2 his3::loxP/HIS3 Klrho5::kanMX/KIRHO5</i>	this study
KHO371	- <sup>2</sup>	<i>MATa/MATalpha ura3/URA3 leu2/LEU2 his3::loxP/HIS3 Kldck1::kanMX/KIDCK1</i>	this study
KHO384	- <sup>2</sup>	<i>MATa/MATalpha ura3/URA3 leu2/leu2 his3::loxP/HIS3 Klrho5::kanMX/KIRHO5 Klgpr1::ScLEU2/KIGPR1</i>	this study
KHO393	- <sup>2</sup>	<i>MATa/MATalpha ura3/URA3 leu2/LEU2 his3::loxP/HIS3 Klsch9::kanMX/KISCH9</i>	this study
KHO401	- <sup>2</sup>	<i>MATa/MATalpha ura3/URA3 leu2/LEU2 his3::loxP/his3::loxP Klsch9::kanMX/KISCH9 Klrho5::SpHIS3/KIRHO5</i>	this study
KHO402	- <sup>2</sup>	<i>MATa/MATalpha ura3/URA3 leu2/leu2 Klgpr1::ScLEU2/KIGPR1</i>	this study
KI017/IDP1mRub	KI927	<i>MATalpha ura3 leu2 his3::loxP ku80::loxP IDP1-mRuby-kanMX</i>	this study
KMO30-4A	MKL237	<i>MATalpha ura3 leu2 MYO1-mCherry-ScURA3 GFP-RHO5-SkHIS3</i>	this study
KMO30-6D	MKL238	<i>MATa ura3 leu2 his3::loxP MYO1-mCherry-ScURA3 GFP-RHO5-SkHIS3</i>	this study
KMO31-4B	MKL251	<i>MATa ura3 leu2 his3::loxP GFP-RHO5-SkHIS3 IDP1-mRuby-kanMX</i>	this study
KMO32-5D	MKL270	<i>MATalpha ura3 his3::loxP leu2::pRRO297-LEU2 DCK1-GFP-SkHIS3</i>	this study
KMO33-8A	MKL271	<i>MATa ura3 his3::loxP leu2::pRRO297-LEU2 LMO1-GFP-SkHIS3</i>	this study

<b><i>Saccharomyces cerevisiae</i> strains</b>			
DAJ138	Os1649	<i>MATa/MATalpha ura3-52/ura3-52 leu2-3,112/leu2-3,112 his3-11,15/his3-11,15 sch9::SkHIS3/SCH9 rho5::kanMX/RHO5</i>	(Schmitz et al., 2015)
HD56-5A	Os5	<i>MATalpha ura3-52 his3-11,15 leu2-3,112</i>	(Kirchrath et al., 2000)
HOD342-6D	Os1483	<i>MATalpha ura3-52 his3-11,15 leu2-3,112 rho5::SpHIS5</i>	this study

<sup>1</sup> All strains listed in this part of the table were *K. lactis* so that the prefix "KI" was omitted for all gene names given and only genes from other species are indicated as such.

<sup>2</sup> Diploid *K. lactis* strains are not kept in glycerol stocks (and therefore have no collection number), due to their tendency to sporulate even in rich medium. As an exception, heterozygous diploids with deletions in essential genes are held in stock.

**Table S2. Vectors and plasmids used in this study \***

Plasmid	Features	References
YCplac111	centromeric vector with <i>LEU2</i> as selection marker in <i>S. cerevisiae</i>	(Gietz and Sugino, 1988)
YEp181JJH	multicopy vector with <i>LEU2</i> as selection marker in <i>S. cerevisiae</i> , and a modified polylinker; derived from YEplac181	(Gietz and Sugino, 1988)
pCXs22	triple shuttle vector for <i>E. coli/S. cerevisiae/K. lactis</i> ; <i>CEN/ARS</i> for <i>S. cerevisiae</i> , multicopy for <i>K. lactis</i> , <i>ScURA3</i> as selection marker for both yeasts	(Heinisch et al., 2010)
pCse24	triple shuttle vector for <i>E. coli/S. cerevisiae/K. lactis</i> ; <i>CEN/ARS</i> for <i>S. cerevisiae</i> , multicopy for <i>K. lactis</i> , <i>ScLEU2</i> as selection marker for both yeasts	(Heinisch et al., 2010)
pUK1921	<i>E. coli</i> cloning vector conferring kanamycin resistance	(Heinisch, 1993)
pUG6	template vector for PCR-based deletions carrying the <i>kanMX</i> marker cassette	(Gueldener et al., 2002)
pUG27	template vector for PCR-based deletions carrying the <i>SpHIS5</i> marker cassette	(Gueldener et al., 1996)

Table S2. continued

pFA6a	GFP-SkHIS3	template vector for PCR-based GFP fusions carrying the <i>SkHIS3</i> marker cassette	(Longtine et al., 1998)
pKT178-mRuby		template vector for PCR-based mRuby fusions carrying the <i>kanMX</i> marker cassette	(Lee et al., 2013)
pJJH955L		template vector for PCR-based deletions carrying the <i>ScLEU2</i> marker cassette	(Heinisch et al., 2010)
pJJH1409		plasmid obtained by gap repair of an erroneous <i>KIDCK1</i> PCR clone; based on pCse24	this study
pJJH1524		template vector for PCR-based mCherry fusions carrying the <i>kanMX</i> marker cassette	this study
pJJH1525		template vector for PCR-based mCherry fusions carrying the <i>SkHIS3</i> marker cassette	this study
pJJH1619		template vector for PCR-based GFP fusions carrying the <i>kanMX</i> marker cassette	this study
pJJH1620		template vector for PCR-based GFP fusions carrying the <i>SkHIS3</i> marker cassette	this study
pJJH2600L		integrative <i>KILEU2</i> vector with polylinker and blue/white screen in <i>E. coli</i>	this study
pJJH2751		integrative <i>KILEU2</i> vector encoding a KILifeAct-mRuby fusion expressed under the control of the <i>ScPFK2</i> promoter in conjunction with a GFP-KIRho5 fusion expressed from its native promoter	this study
pJJH2759		<i>KIRHO5</i> in YEp181JJH	this study
pJJH2760		<i>KIRHO5</i> <sup>Q69H</sup> in YEp181JJH	this study
pJJH2917		integrative <i>KILEU2</i> vector with <i>KICDC42</i> <sup>G12V</sup> under its native promoter	this study
pJJH2918		integrative <i>KILEU2</i> vector with <i>KICDC42</i> under its native promoter	this study
pMMO5		integrative <i>KILEU2</i> vector with <i>KIRHO5</i> coding sequences flanked by its native regions	this study
pMMO6		integrative <i>KILEU2</i> vector with <i>KILMO1</i> coding sequences flanked by its native regions	this study
pMMO7		integrative <i>KILEU2</i> vector with <i>KIDCK1</i> coding sequences flanked by its native regions	this study
pMMO22		integrative <i>KILEU2</i> vector with <i>GFP-CDC42</i> expressed from the <i>ScPFK2</i> promoter	this study
pRRO297		integrative <i>KILEU2</i> vector with a nuclear localization sequence fused to mCherry expressed from the <i>ScPFK2</i> promoter	gift from Rosaura Rocio

\* Complete sequences of all plasmids listed are available upon request.

**Table S3. Deletions tested for synthetic lethality with *Klrho5***

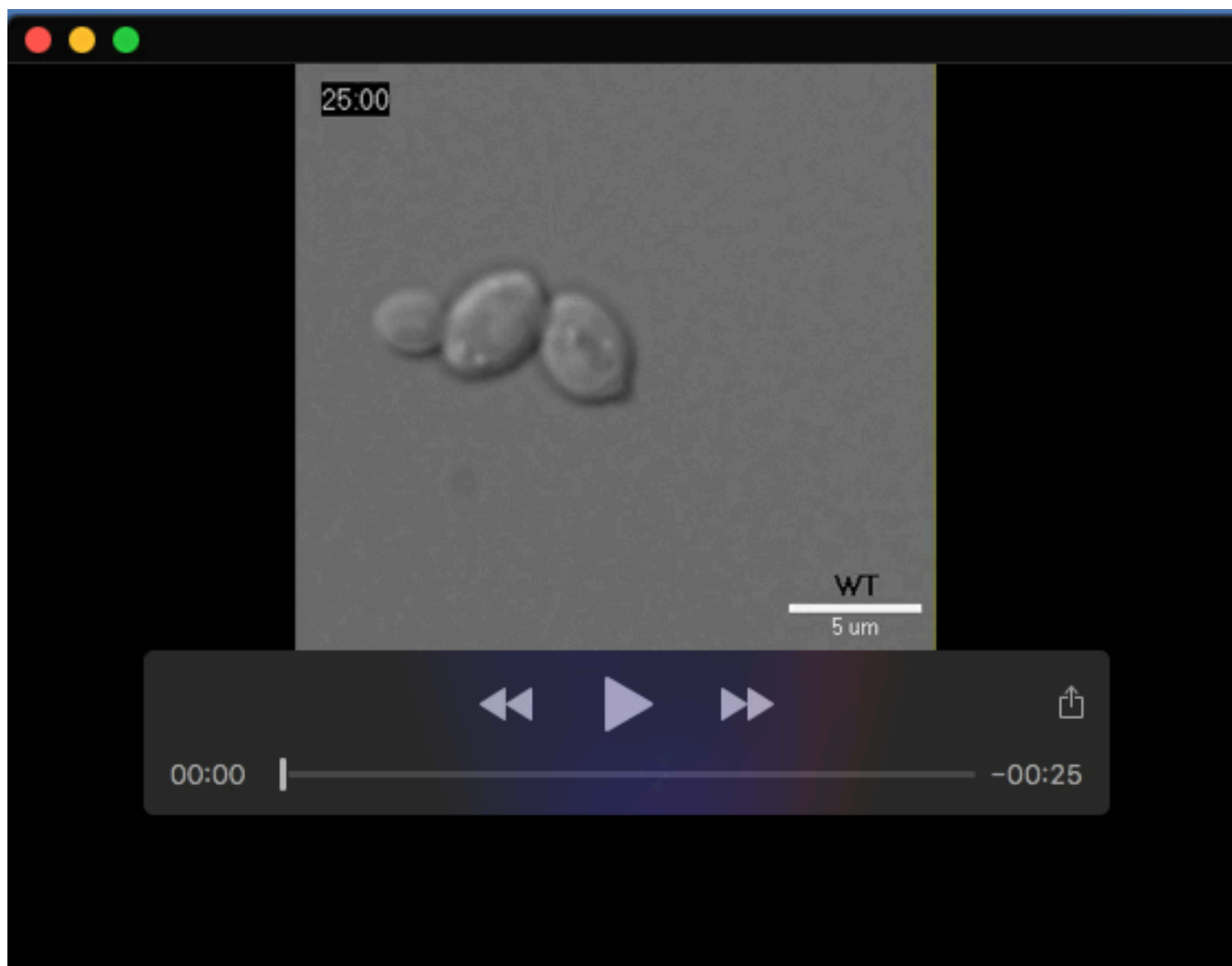
Strain <sup>1</sup>	Deleted gene ::marker	Function of wild-type protein <sup>2</sup>	Double deletion with <i>Klrho5</i> <sup>3</sup>
KHO341	<i>Klsnf1::kanMX</i>	carbohydrate signaling	viable
KHO293	<i>Klsch9::ScLEU2</i>	nutrient signaling	viable
KHO291	<i>Klgpr1::ScLEU2</i>	nutrient signaling	viable
KHO354	<i>Klzwf1::ScLEU2</i>	pentose phosphate pathway	viable
KHO344	<i>Klrpe1::SpHIS5</i>	pentose phosphate pathway	viable
KMO24	<i>Kltal1::ScLEU2</i>	pentose phosphate pathway	viable
KHO381	<i>Klpor1::SkHIS3</i>	mitochondrial ion channel (VDAC)	viable
KHO316	<i>Klsod1::ScLEU2</i>	oxidative stress response	viable
KHO314	<i>Klsod2::SpHIS5</i>	oxidative stress response	viable
KHO377	<i>Klmpk1::ScLEU2</i>	cell wall integrity signaling	viable
KHO379	<i>Klbck1::kanMX</i>	cell wall integrity signaling	viable
KHO378	<i>Klrlm1::ScURA3</i>	cell wall integrity signaling	viable
KHO276	<i>Klpil1::ScHIS3</i>	eisosome formation	viable
KHO277	<i>Kllsp1::ScLEU2</i>	eisosome formation	viable
KHO338	<i>Klmyo1::kanMX</i>	cytokinesis	viable
KMO17	<i>Klhof1::ScURA3</i>	regulation of cytokinesis	viable
KHO368	<i>Kltdp1::ScLEU2</i>	DNA repair	viable

For all listed deletions, the entire open reading frames were substituted for the indicated heterologous markers by homologous recombination with the respective cassettes flanked by target sequences primarily added by PCR. All strain manipulations were performed exclusively in the congenic strain series used in this work and first described in (Heinisch *et al.*, 2010), taking advantage of the *ku80::loxP* deletion. Most deletions were constructed in the course of this study. Published work is available for *Klsnf1* (Rippert *et al.*, 2017), *Klzwf1* (Heinisch *et al.*, 2020), *Kltal1* (Jacoby *et al.*, 1993), *Klmpk1* (Kirchrath *et al.*, 2000), *Klbck1* (Jacoby *et al.*, 1999), *Klmyo1* and *Klhof1* (Rippert *et al.*, 2014). For works published prior to 2010 with other *K. lactis* strains, deletions were reconstructed in the congenic strain series, herein.

<sup>1</sup> Listed are the diploid strains heterozygous for both the respective deletion and a *Klrho5* allele, which were sporulated to test for synthetic lethality by tetrad analyses. All spores were allowed to germinate on rich medium (YEED) for at least three days at 30°C.

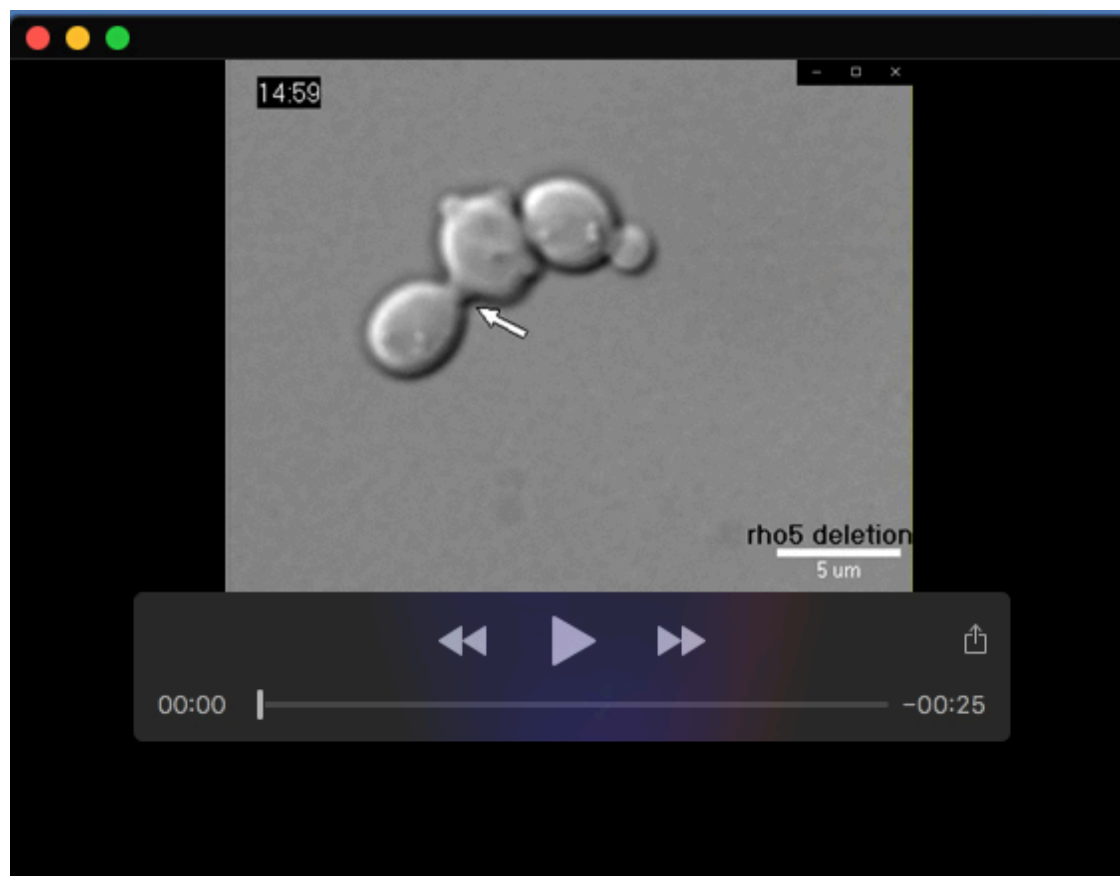
<sup>2</sup> Functions of the proteins encoded by the respective wild-type genes were either studied in the works cited above or deduced from those of their *S. cerevisiae* homologs.

<sup>3</sup> A *Klrho5::kanMX* deletion allele was used throughout to test for synthetic lethality, except for the crosses with *Klsnf1::kanMX* and *Klbck1::kanMX*, for which a *Klrho5::SkHIS3* allele was employed.

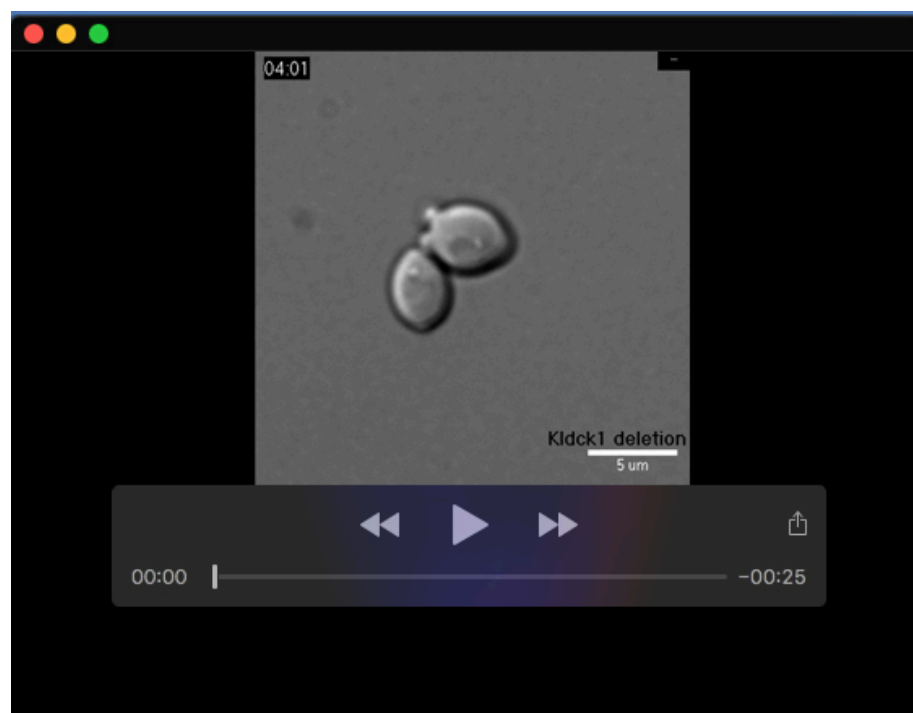


**Movie 1.** Time-lapse images following budding of wild-type (CBS2359) cells for 12.5 hours. Pictures were taken every five minutes with the 100fold magnification lens. In the movie, the time between the pictures was set to 1 second. The scale bar is 5  $\mu\text{m}$ .

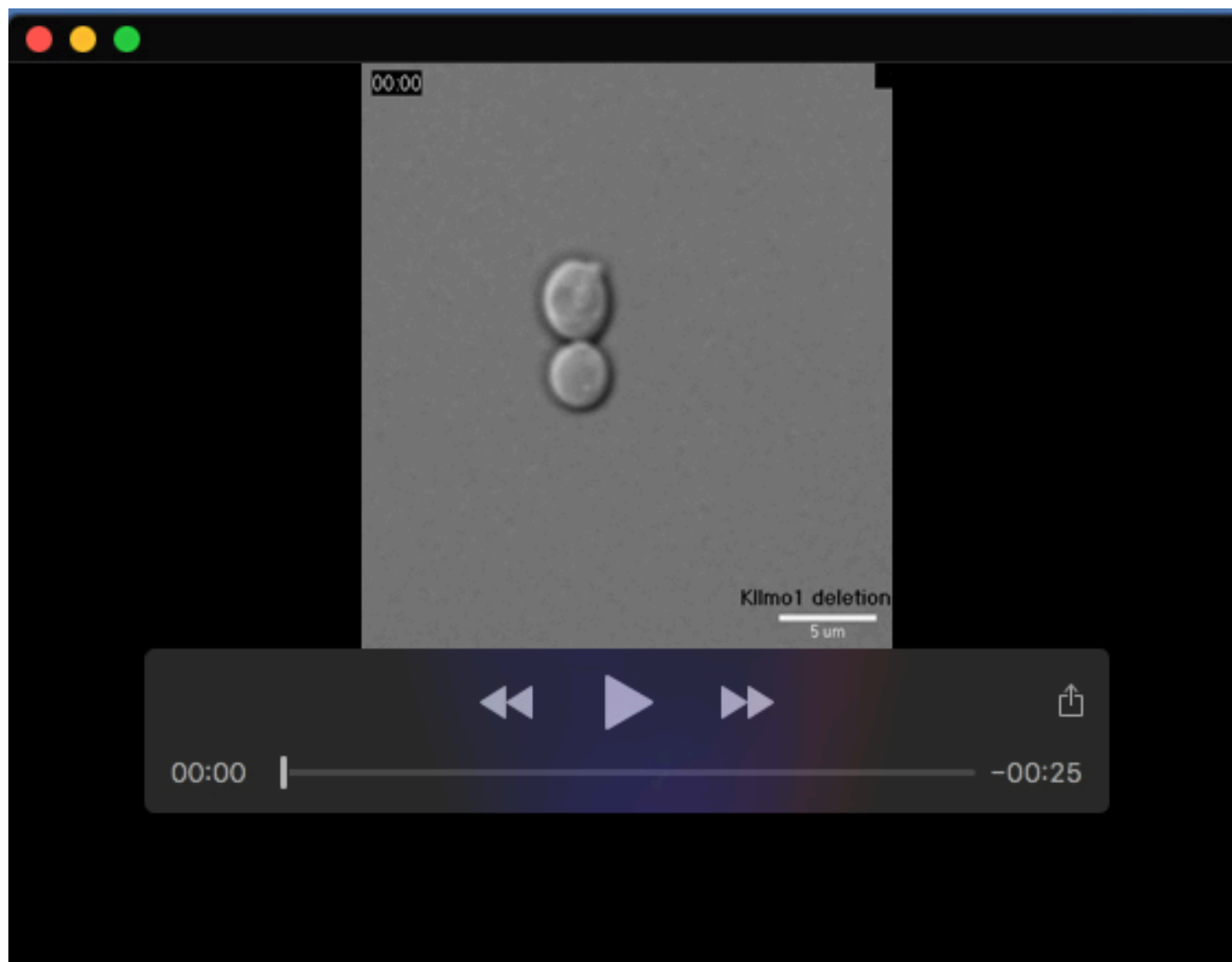




**Movie 2.** Time-lapse images following budding of *Klrho5* (KHO208-8B) cells for 8 hours. Positions of budding resulting in protruding bud scars are indicated by arrows. Magnification, compression for time lapse, and scale bar are as described in the legend to Movie 1.



**Movie 3.** Time-lapse images following budding of *Kldck1* (KHO.01-14C) cells for 8 hours and pictures were taken every two minutes. Positions of budding resulting in protruding bud scars are indicated by arrows. Magnification and scale bar are as described in the legend to Movie 1.



**Movie 4.** Time-lapse images following budding of *Kllmo1* (KHO.03-1D) cells for 4.5 hours and pictures were taken every five minutes. Positions of budding resulting in protruding bud scars are indicated by arrows. Magnification, compression for time lapse, and scale bar are as described in the legend to Movie 1.

## References:

- Heinisch JJ, Buchwald U, Gottschlich A, Heppeler N & Rodicio R (2010) A tool kit for molecular genetics of *Kluyveromyces lactis* comprising a congeneric strain series and a set of versatile vectors. *FEMS Yeast Res* **10**: 333-342.
- Heinisch JJ, Knuesting J & Scheibe R (2020) Investigation of heterologously expressed glucose-6-phosphate dehydrogenase genes in a yeast *zwf1* deletion. *Microorganisms* **8**. doi: 10.3390/microorganisms8040546
- Jacoby J, Hollenberg CP & Heinisch JJ (1993) Transaldolase mutants in the yeast *Kluyveromyces lactis* provide evidence that glucose can be metabolized through the pentose phosphate pathway. *Mol Microbiol* **10**: 867-876.
- Jacoby JJ, Kirchrath L, Gengenbacher U & Heinisch JJ (1999) Characterization of *KIBCK1*, encoding a MAP kinase kinase kinase of *Kluyveromyces lactis*. *J Mol Biol* **288**: 337-352.
- Kirchrath L, Lorberg A, Schmitz HP, Gengenbacher U & Heinisch JJ (2000) Comparative genetic and physiological studies of the MAP kinase Mpk1p from *Kluyveromyces lactis* and *Saccharomyces cerevisiae*. *J Mol Biol* **300**: 743-758.
- Rippert D, Backhaus K, Rodicio R & Heinisch JJ (2017) Cell wall synthesis and central carbohydrate metabolism are interconnected by the SNF1/Mig1 pathway in *Kluyveromyces lactis*. *Eur J Cell Biol* **96**: 70-81.
- Rippert D, Heppeler N, Albermann S, Schmitz HP & Heinisch JJ (2014) Regulation of cytokinesis in the milk yeast *Kluyveromyces lactis*. *Biochim Biophys Acta* **1843**: 2685-2697.